BRANDFORS
K 2016:4/1

Validation data for room fire models; Experimental background

Alexandra Byström, Johan Sjöström, Johan Andersson, Ulf Wickström

Brandforsk

BRANDFORSK 2016:4
IS BN 978-91-88349-56-9

Abstract

Validation data for room fire models: Experimental background

A series of room fire tests for enclosures with different wall materials have been conducted for the purpose of supplying validation data for enclosure fire models. The wall materials are varied between light weight concrete, mineral wool insulation, bare 3 mm steel, and finally insulated steel. All tests used a propane gas burner with a well-defined mass flux as a fire source. Temperatures of thermocouples and plate thermometers were measured as well as oxygen concentrations in the opening. For some tests the heat release rate (by oxygen consumption calorimetry) as well as O_2, CO_2 and CO concentrations were measured in addition.

This report describes the instrumentation, fire scenarios, enclosure materials, and results from all the tests. All results are readily available as spreadsheet data for downloading. The report also contains short description showing the influence of different factors such as wall materials, heat release rates and burner placements.

Key words: Room fires; validation; experiments; thermal properties; walls

SP Technical Research Institute of Sweden

SP Report 2016:54
ISBN 978-91-88349-56-9
ISSN 0284-5172
Borås 2016

Contents

Preface

This is an experimental report for a project labelled *Development and validation of simple and practical models from calculation of fire gas temperatures in enclosures* (*Utveckling och validering av enkla och praktiska modeller för beräkning av brangastemperaturer i rum/brandceller* in Swedish). The project is funded by Brandforsk, The Swedish Fire Research Board. A part of the project objective concerns delivery of very well-defined experiments for validation of fire models. The idea is to use a known fuel load in terms of a mass flux controlled propane burner and run several experiments using different types of materials for the compartment boundaries. The data can be used for validation of different models by other researchers and is therefore freely available to download as spreadsheet data.

Light weight concrete, mineral wool, steel and insulated steel is used in the four test series presented here. In addition, for the first run of LWC the material contained 40 % moisture which had a noticeable influence on the fire temperatures.

A second part of the project is published in a separate report where a simple one-zone model is validated against the data sets (Byström, Sjöström, Anderson, & Wickström, 2016).

Summary

Four test series of room fires with different surrounding materials were conducted and described in this report. The intention of the work was to create data for validation of enclosure fire models. The data is now freely available to download in spreadsheet format, (Sjöström & Wickström, 2016).

An enclosure with inner dimensions 2700 mm long, 1800 mm wide and 1800 mm high and with an opening 600 mm wide and 1500 mm high with different surrounding materials was used. In all experiments all surrounding boundary structures, walls, ceiling and floor were the same. The only heat source was a propane burner placed either at the rear wall or in the middle of the room. Temperature was measured with several thin thermocouples and plate thermometers in the fire gases and within the walls. In addition, concentrations of gas species were measured in the opening at different heights .

This report highlights some of the results. All are not shown but are available for anybody for further analyses as specified above.

1 Introduction

Modelling and simulating compartment fires in different geometries is essential in fire risk assessments of structures. Models have been developed since decades back from hand calculations (many of which are presented in (Karlsson & Quintiere, 2000)), via one- or two-zone models (Jones, 1983) and simple numerical tools (Wade, 2008) to more sophisticated fluid dynamics codes such as the Fire Dynamics Simulator, FDS, (McGrattan, Baum, & Rehm, 1998). The pioneering work by Magnusson and Thelandersson in the 60s and 70s (Magnusson & Thelandersson, 1970) formed the basis for most of the models on natural post-flashover fires and has been reformulated into parametric fire curves in the Eurocodes (ENV 1991:1-2, 1995), (Wickström, 1985). Plenty of activities are ongoing for improving models including both fluid dynamics codes (McGrattan, Peacock, & Overholt, 2014) and simple models, both in the pre- (Byström, Fire temperature development in enclosures: Some theoretical and experimental studies, 2013) and post-flashover (Evegren & Wickström, 2015) phase. An overview can be found in the recently published book by Wickström (Wickström, 2016).

For the usability and development of these models there is always a need for validation data. Validation is aimed at different levels of complexity and the therefore different types of experimental data are needed. This study aims at producing data for validation of models which take into account the thermal behaviour of the enclosure materials. The burning rate of fuel usually increases with time and so does the enclosure boundary surfaces temperatures, which makes comparison with simulations very difficult. Therefore, this set of experiments are all performed using a gas burner with a known mass flux output, independent of the temperatures in the enclosure and the thermal exposure of the heat source. The report summarizes twelve experiments in four test series. All the data can be downloaded in spreadsheet format with diagrams (Sjöström & Wickström, 2016). The report also highlights some of the differences between the tests.

2 Method

2.1 Test objects

The inner dimensions of the structure were such as to represent an office in scale 3:4, see Figure 1, the real dimensions were 1800 mm in width and height and 2700 mm in length. Centrally on one of the short ends an opening representing a door was created with 1500 mm in height and 600 mm in width. The materials in and thickness of the walls changed between the test series.

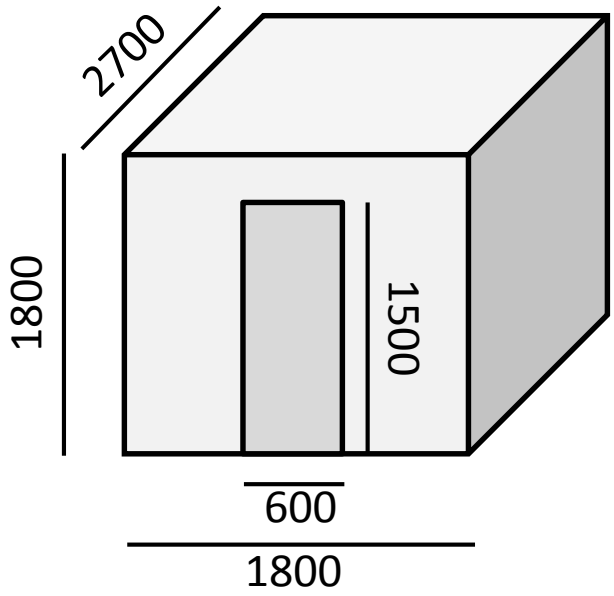

Figure 1. Inner dimensions of the test objects in mm.

Figure 2. The propane sand diffusion gas burner used in all tests.

2.2 Wall materials and series

The fire source consists of a non-premixed propane burner with a controlled mass flux. The mass flux is calibrated such that it represents a specific heat release rate for free burning conditions, i.e. it has been tested under a calibrated oxygen consumption calorimeter where the mass flow is correlated to total heat release rate (HRR). This system has previously been used in tunnel fire experiments (Ingason, Appel, Li, Lundström, & Becker, 2014). The burner is a 300 mm by 300 mm square burner of stainless steel, see Figure 2. The gas inlet is through the wall close to the bottom of the burner and half the volume is filled with gravel (~10-20 mm stones). Five different fire scenarios were defined, see Table 1.

Four test series are reported here. They are all conducted using a mass flux controlled gas burner in enclosures with the same inner dimensions and opening. Each series represent different thermal properties of the enclosing walls, see Table 1.

Table 1. Overview of the tests. In all but test A3 the burner is placed in the centre of the floor.

Test	Fire intensity (kW)	Material	Comment
A1	1000	Light Weight Concrete (LWC)	
A2	500	LWC	
A3	1000	LWC	1000 kW – placed at back wall
A4	$250 + 20 \cdot t$, $t<50$ 1250, $t \geq 50$, t in minutes	LWC	
A5	1000	LWC	As A1 but free water gone
B1*	1000	Steel insulated on inside	
B2*	1000	Steel insulated on inside	Same as B1
C1	500	Unisulated steel	
C2	1000	Unisulated steel	
C3	$200 + 60 \cdot t$, $t<17.5$ 1250, $t \geq 17{,}5$, t in minutes	Unisulated steel	Ramp to 1250 kW
D1	1000	Steel insulated on outside	
D2	1000	Steel insulated on outside	Same as D1

* The insulation in this test series was on the inside of the steel structure and the inner dimensions were therefore reduced to 1700x1700x2600 mm^3 with a door opening of 1450x600 mm^2.

2.2.1 Test series A – lightweight concrete

Figure 3. Test object A, enclosure made of 100 mm lightweight concrete, walls, ceiling as well floor.

Test series A was conducted on a structure from light weight concrete (LWC) of type Siporex with a thickness of 100 mm. Figure 3 shows a photo of the enclosure supported by a steel frame. The density of the material was measured before testing. Also, two samples from the same batch were used to measure moisture content by drying in a furnace at 105 °C during 24 h. The density of these samples were 754 and 767 kg/m^3 containing 35 and 42 % moisture (as water content/dry material), respectively. More details are found in Table 2

The concrete was also tested, repeatedly, for specific heat and thermal conductivity using Transient Plane Source (Gustafsson, 1991) at room temperature both before and after exposure to the five fire tests.

Table 2. Thermal material properties of the lightweight concrete in test series 1. The values within parentheses denote the spread between measurements and specimens. The data in the "after fire exposure"-column represent data measured on samples from the actual enclosure after the final test.

Property	Before fire exposure - wet	After fire exposure - dry
Density (kg/m^3)	760 (±7)	
Moisture content (%)[1]	39 (±3)	-
Specific heat (J/kgK)	851 (±19)	835 (±16)
Thermal conductivity at room temperature (W/mK)	0.330 (±0.009)	0.166 (±0.006)

[1] mass of water/mass of dry material.

The walls and ceiling in the enclosure was instrumented by insulated plate thermometers (insPT – hereafter referred to as PT) described in (Sjöström & Wickström, 2013) and previously used in many field experiments (Sjöström, Amon, Appel, & Persson, 2015) (Sjöström & Andersson, 2013). The PT are positioned a fourth of the distance from adjacent walls/floor/ceiling as well as in the centre and are indicated as squares on all inner surfaces in Figure 4. An additional PT is positioned 1000 mm from the door opening at 600 above floor level.

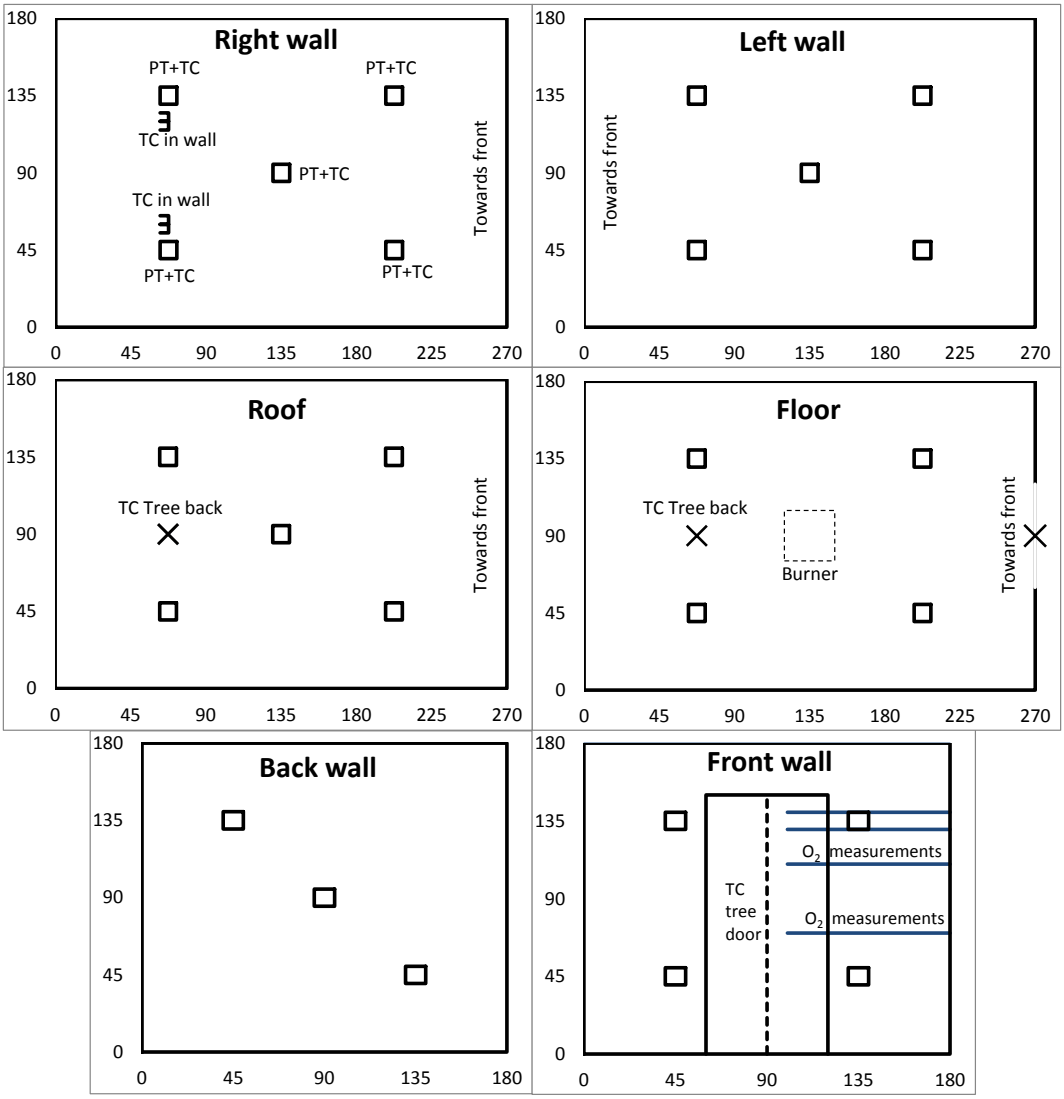

Figure 4. The instrumentation at the inside of the enclosure for test series A. The distances are in cm. All squares are PTs unless stated otherwise. The back TC tree spans from ceiling to floor and the door TC tree from top to bottom of the opening. O_2 gas concentration measurements were performed in the opening at distances 100, 200, 400 and 800 mm from the top of the opening. The inlet of the pipes were 15 cm from the centre line.

0.5 mm welded type K thermocouples (TC) are placed next to the PT on the right wall. Within the right wall there are also TC inserted at heights of 600 and 1200 mm at a depths of 25, 50 and 75 mm. See Figure 5 for the configuration of the TC in the LWC wall.

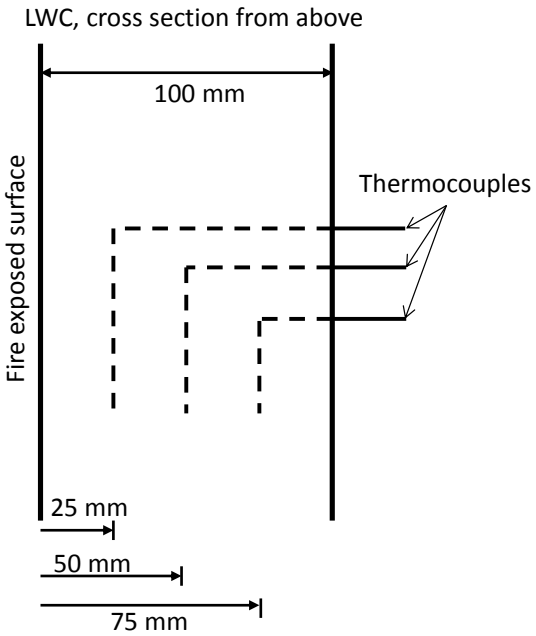

Figure 5. The configuration of the TC in the LWC wall in the right wall, 675 mm from the back wall at two heights, 600 and 1200 mm above floor level.

Two TC trees are also used with 300 mm spacing from floor to ceiling, one in the back region of the room and one in the door opening. The door TC tree is also equipped with measuring points at 150 and 450 mm from the top of the door opening. For the A-series the TC tree were welded 25 mm TC. These did not function within the enclosure except when changed for the last test, A5. For series B-D the TC tree used 1 mm shielded thermocouples instead.

O_2 gas concentrations measurements are measured in the opening a distance 100, 200, 400 and 800 mm from the top of the opening. The inlet of the pipes were situated 150 mm from the centreline of the opening.

In Test series A fire intensities 1 to 4 were run in consecutive order according to table 1. Thereafter, when the concrete was dry, fire intensity 1 was performed again.

The Test series A was conducted in a small burn hall with dimensions 14 × 8 × 20 m. The combustion gases were evacuated in the ceiling but no oxygen consumption calorimetry was conducted to evaluate heat release rate. The room was almost symmetric from looking from the left or right wall of the test object. However, air inlet was in the floor level on the left hand side.

2.2.2 Test series B – steel structure insulated on the inside

Test series B was conducted on a mild steel structure with 3 mm thickness, 7850 kg/m^3. The inner dimensions of the steel enclosure were identical to test series A (see Figure 1). However, 50 mm of stone wool board covered the inside walls. Thus, the width/length/height of the inner surfaces in test series B are 100 mm smaller compared to series A, giving dimensions of 1700/2600/1700 mm, respectively.

The stone wool had a nominal density of 200 kg/m^3 and a nominal room temperature conductivity of 0.04 W/mK. Porous materials exhibit a temperature dependence on the thermal conductivity, analysed in (Sjöström & Jansson, 2012). The instrumentation of this test series was instrumented as test series C and D, shown in Figure 6, only that the enclosure surfaces were shifted 50 mm by the insulation boards. In addition, the right wall was monitored from outside by an IR-camera. CO, CO_2 and O_2 gas concentrations

were measured 100, 200 and 800 mm from the opening top. The CO and CO_2 measurement equipment were not available for the A series.

The TC tree temperatures were measured using 1 mm shielded thermocouples.

For series B, C and D, all the hot gases were collected in a large hood and analysed in an oxygen consumption calorimeter. This calorimeter measures the total HRR based on the consumed oxygen. It also measures the convective HRR, defined as the energy used to heat the gases from the fire. This is measured by analysing the gas flow and its temperature.

2.2.3 Test series C – uninsulated steel structure

Test series C was conducted on the same steel structure as test series B but without any insulation. The instrumentation is shown in Figure 6, the right wall was monitored by an IR-camera and the gas measurements were performed as in test C.

2.2.4 Test series D –steel structure insulated on the outside

Test series D was conducted on the same steel structure as test series C but with 50 mm of 200 kg/m^3 insulation boards on all *external* surfaces. The same instrumentation as test series C was used.

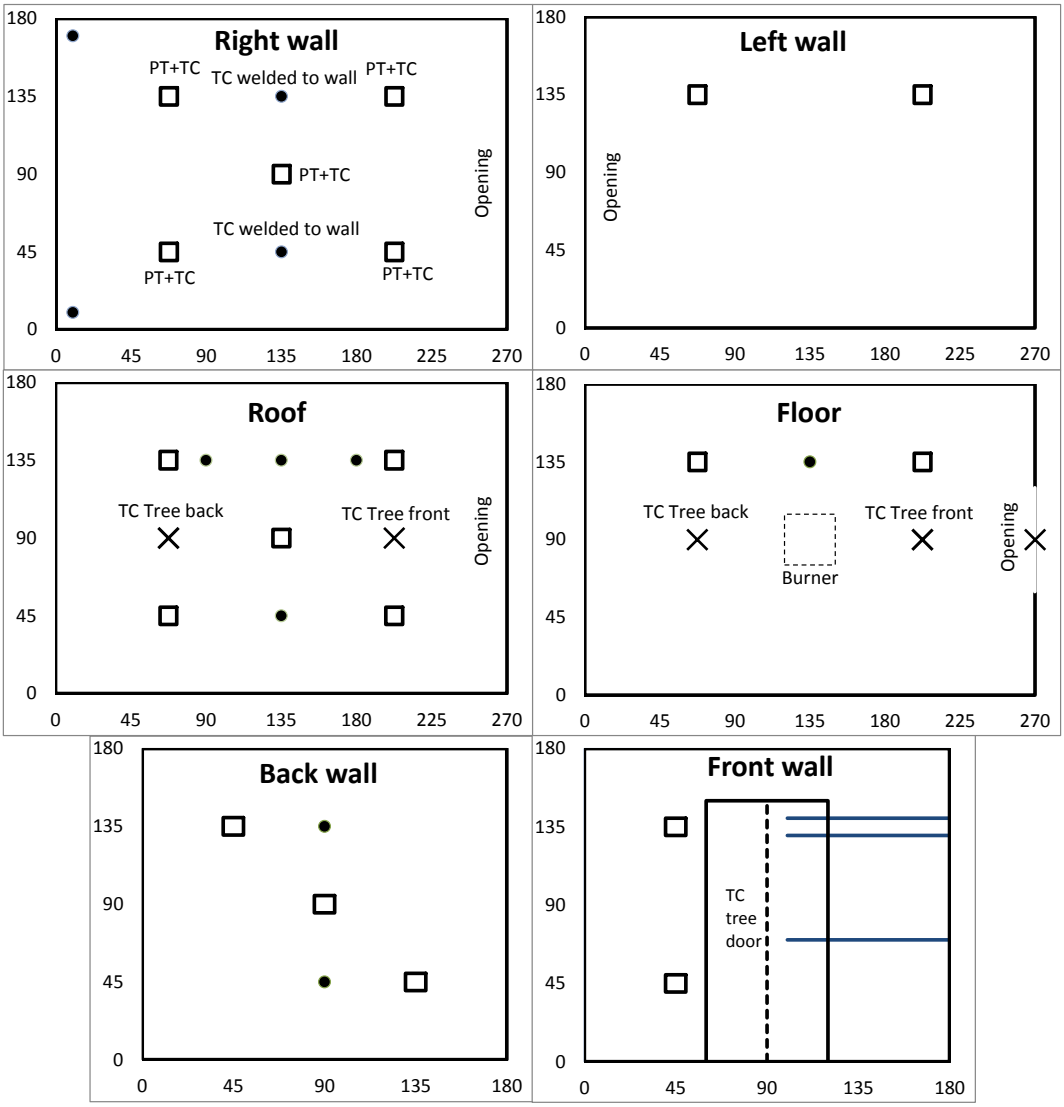

Figure 6 . The instrumentation at the inside of the enclosure for test series B, C and D. The distances are in cm. Squares are PTs only unless stated otherwise. Black points are TCs fixed to steel enclosure structure. The tubes in the door opening measure CO, CO_2 and O_2 gas concentrations at 100, 200 and 800 mm from the top of the opening.

3 Results

All results are available to download as spreadsheet data. Below we present some key aspects of the results. For each test, when applicable, we present the time evolution of PT temperatures on the right wall, the PT temperature in the ceiling and the TC tree temperatures in the door opening once equilibrium conditions do not change anymore. In addition, the right wall temperatures (temperature of steel and LWC at different depths).

Some instruments failed during a complete test or during part of a test. This occured primarily for thermocouples in the TC trees and for the gas analysers. The problem with the gas analysers were insufficient cooling traps, which made the values drift after being exposed to too sooty gases after some time through the tests. Thus, for some of the tests data from TC trees or gas concentrations are missing.

For all tests, the temperatures closer to the right wall were higher than those to the left wall. The reason for this is either a small asymmetry of the experimental halls or an intrinsic asymmetry of the burner flame. Analysing the spreadsheet data will give examples of this asymmetry for all tests. Notable, in test series A the difference is larger compared to the other test series.

3.1 Test series A

Test series A were all conducted on the enclosure with LWC walls. The TC trees within the enclosure malfunctioned during Tests A1-A4 so only the opening TC temperatures is shown for these tests.

The O_2 concentrations are generally constant throughout the tests as long as the HRR is constant, even though temperature increases significantly. Generally there is a tendency for a slight increase of the O_2 concentration during the test. However, not all measurement series were completed due to insufficient cooling traps, see the spreadsheet data for details.

Below we display the concentrations at the four different heights for all tests in the A-series. The variations within each data point over the test series it usually ± 1 %.

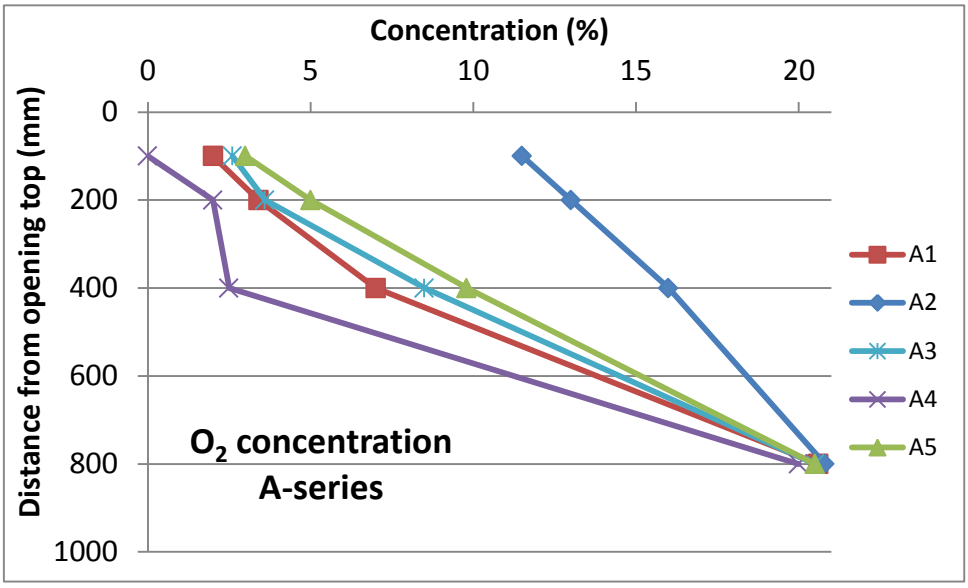

Figure 7. O_2 concentrations at four different heights during tests A1-A5.

The rest of the result from the A-series tests are shown for each test individually below. Not all data is presented but available in the spreadsheet data.

3.1.1 Test A1 - virgin LWC, 1000 kW

The burner was placed in the centre of the enclosure floor and burned at a constant rate of 1000 kW. Despite the symmetric setup the flames in the ceiling actually had a tendency towards the right side of the enclosure. This had a great impact on the temperatures which increased from left to right. A temperature gradient was also noticed in the back to front direction with higher temperatures closer to the opening compared to the back, most significant in the smoke layer. This was noticed both by both TC and PT temperature measurements.

Figure 8. Photo from test A1 – virgin LWC, 1000 kW.

The smoke layer remained constant at half the ceiling height (≈ 900 mm, the centre PT on the walls were partially covered / partially visible) throughout the test, see Figure 8. The PT temperatures of the right wall are shown in Figure 9.

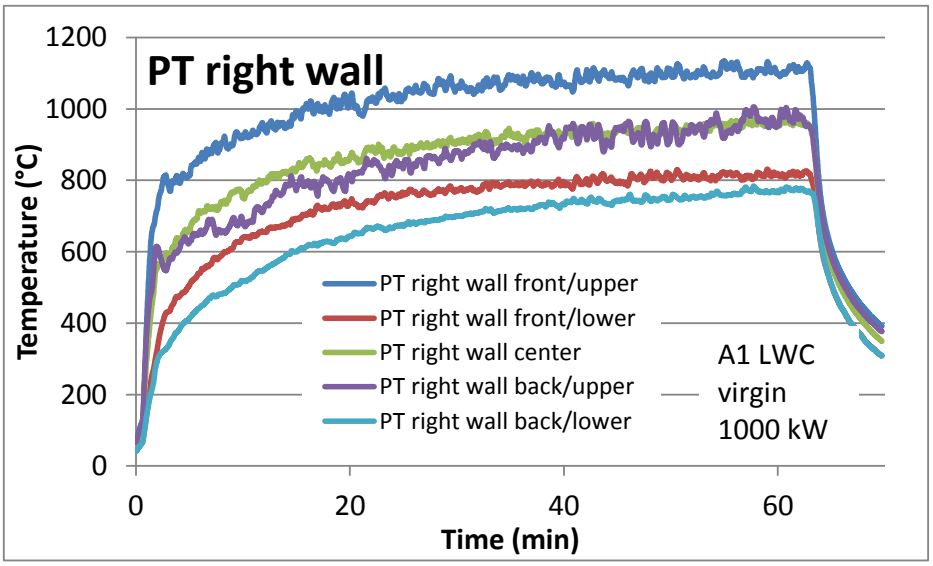

Figure 9. PT temperatures of the right wall in test A1 – virgin LWC, 1000 kW. "Upper" implies the upper part of the enclosure, 1350 mm from floor level. "Lower" implies the lower part, 450 mm from floor. "Back" implies 25 % of the distance from back to front wall, 675 mm from back wall and "front" implies 75 % the same distance, 2025 mm from the back wall, see Figure 4. This is the same throughout the whole report.

The PT temperatures below the gas layer were identical between the left and right wall to within 10 °C on average and 20 °C in the scatter. On the other hand, the temperatures in the hot gas layer were higher on the right side, by more than 100 °C at some positions. The same asymmetry was also noticed for the PT mounted in the ceiling, see Figure 10.

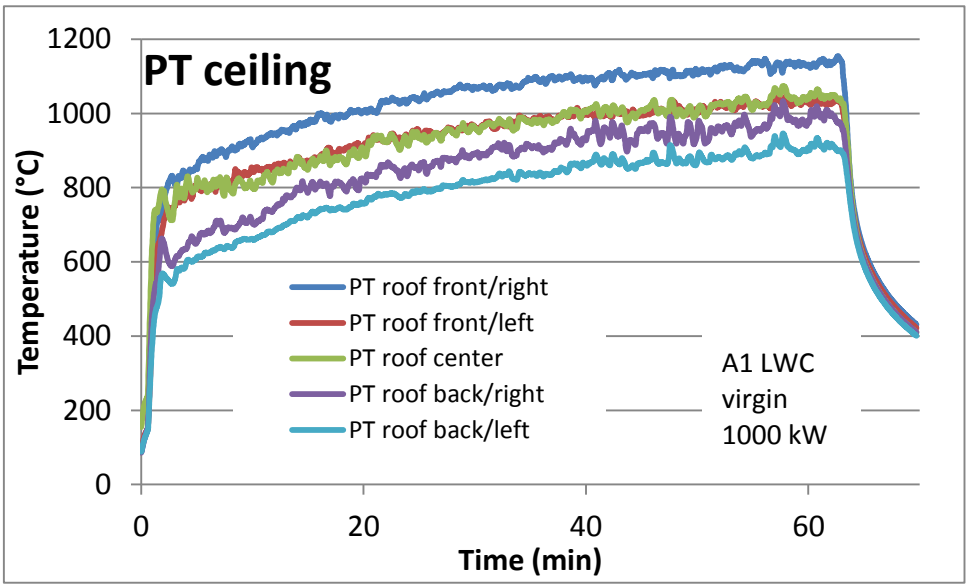

Figure 10. PT temperatures of the ceiling in test A1 – virgin LWC, 1000 kW.

The TC trees within the room malfunctioned during all the tests in the A-series. However, the door opening TC tree functioned and are shown in Figure 11. The equilibrium is taken as a minute average at a time when the temperatures no longer change in time apart from scattering (60 min for test A1). However, even though PT temperatures on the wall had almost stabilized the PT temperatures in the ceiling were still increasing after an hour. Thus, equilibrium conditions were not really met. From the time evolution of the TC temperatures it is nevertheless clear that the TC temperatures almost had reached constant values, see the available data set for more information (Sjöström & Wickström, Dataset: Validation data for room fire models. DOI: 10.13140/RG.2.1.5138.6482, 2016).

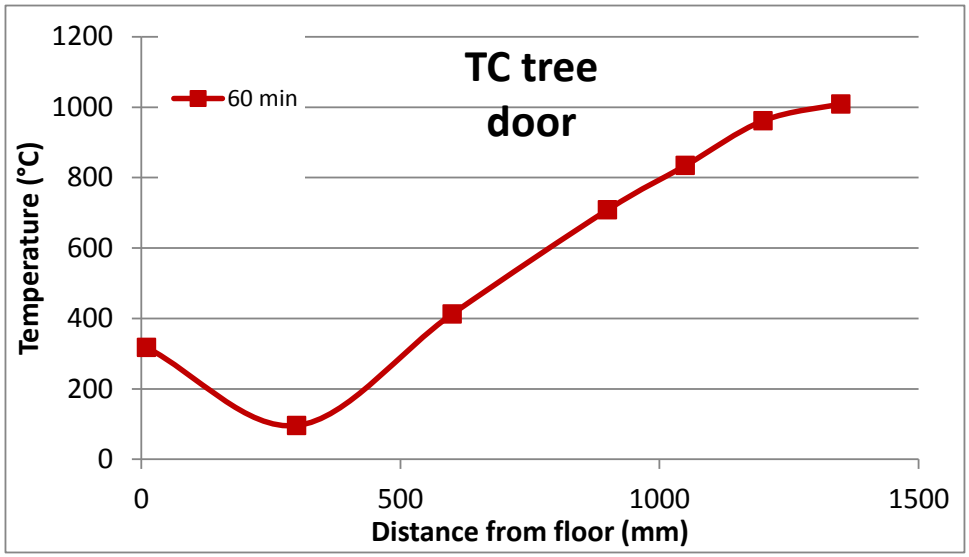

Figure 11. Test A1 – TC tree temperatures in the door opening at equilibrium conditions – virgin LWC, 1000 kW.

Figure 12 shows the TC-measurement inside the wall, see upper left part of Figure 4. The moisture in the LWC keeps the temperatures at 100 °C for a long period of time as a considerable amount of heat is needed to evaporate the water. It is clear that the free water is gone at a depth of 25 mm in the upper part of the wall after 24 minutes when the temperature starts increasing rapidly. Below the hot gas layer the free water evaporates at about 34 minutes.

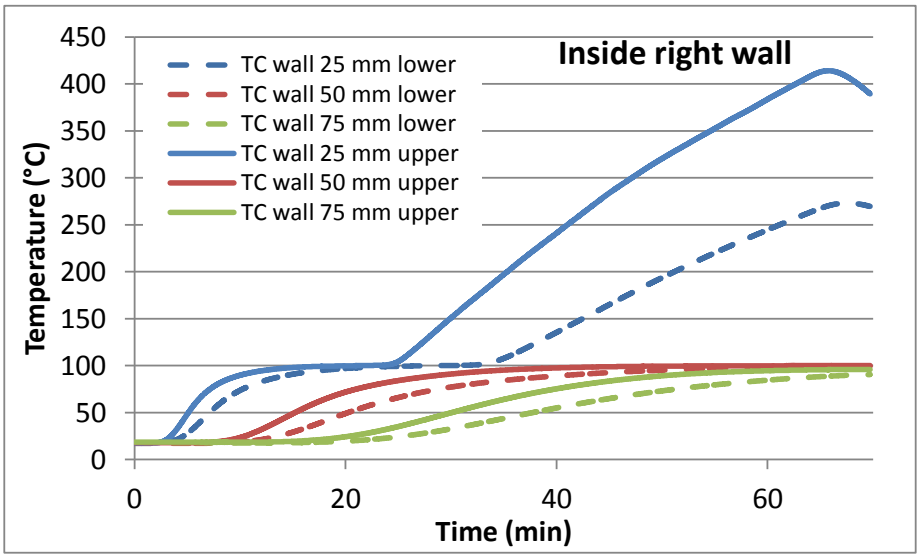

Figure 12. Test A1 - In-depth temperatures of the right wall at heights 1200 mm (upper – solid lines) and 600 mm (lower – dashed lines). The 20, 50 and 75 mm refers to depth from the exposed wall surface.

3.1.2 Test A2 - LWC, 500 kW

This test was identical to test A1 but the HRR of the burner was set to a constant rate of 500 kW throughout the test. In this test, as for all test in series A, the temperatures within the gas layer were higher on the right side. The ceiling PT temperatures differed by as much as 150 °C, PT wall temperatures within the gas layer by almost 100 °C and below

the hot gas layer by only about 10 °C. The PT temperatures on the right wall and the ceiling are shown in Figure 13 and Figure 14, respectively.

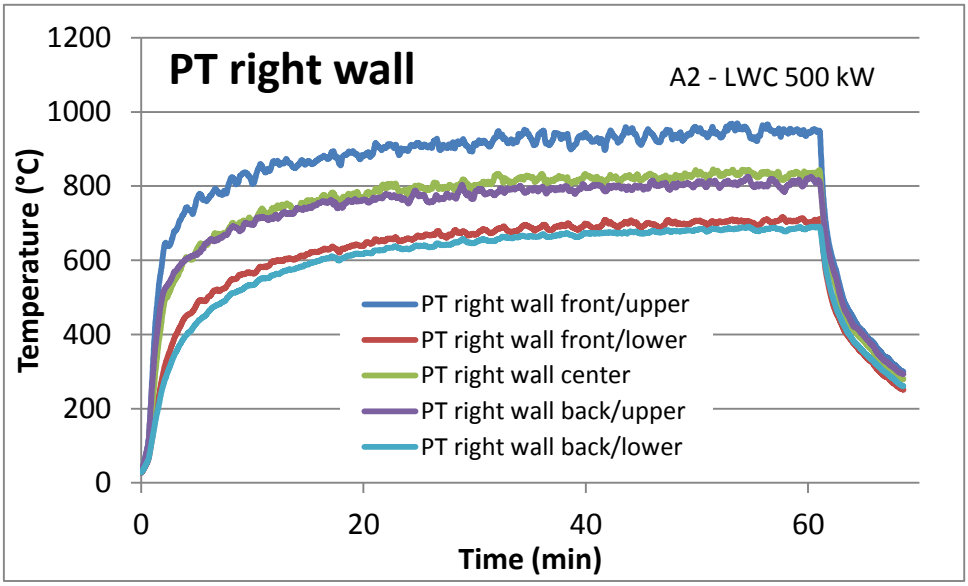

Figure 13. Test A2 - PT temperatures on the right wall.

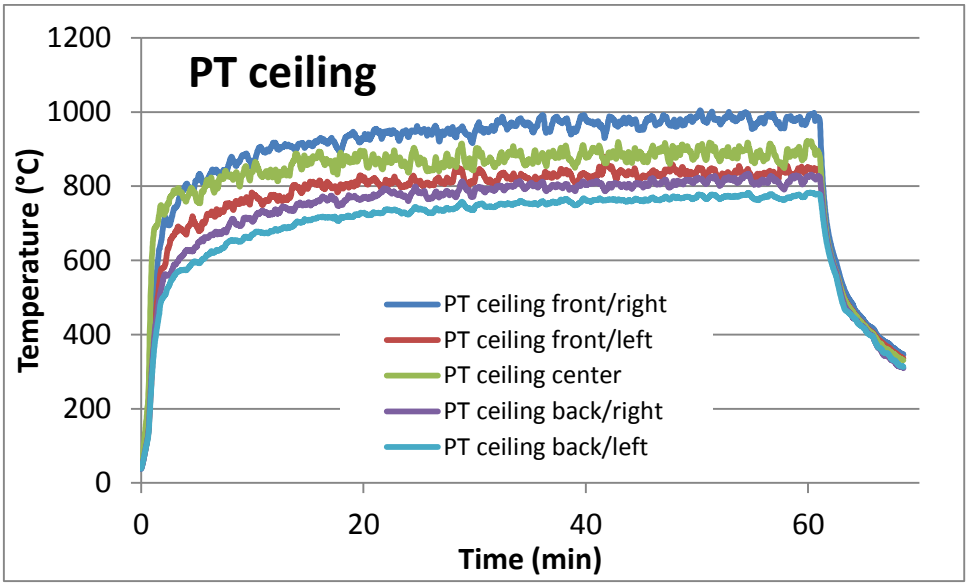

Figure 14. Test A2 - PT temperatures on the ceiling.

The TC tree temperatures in the opening at equilibrium conditions (60 minutes) are shown in Figure 15. The TC temperature exhibits almost a linear dependence with respect to height.

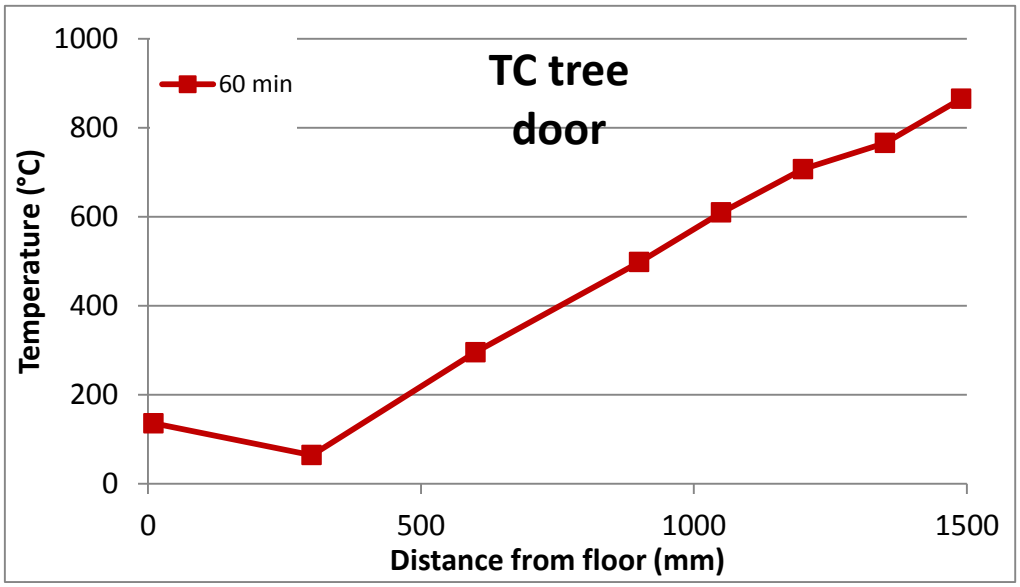

Figure 15. Test A2 – TC tree temperatures in the door opening at equilibrium (60 minutes) – LWC, 500 kW.

The temperatures within the wall show very little effect of free water, see Figure 16.

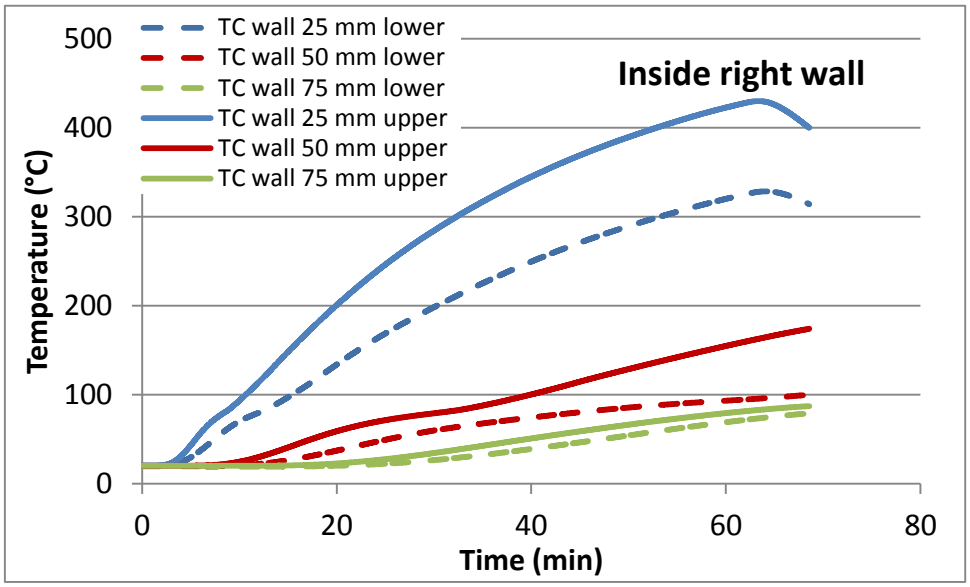

Figure 16. Test A2 - In-depth temperatures of the right wall at heights 1200 mm (upper – solid lines) and 600 mm (lower – dashed lines). The 20, 50 and 75 mm refers to depth from the exposed wall surface.

3.1.3 Test A3 - LWC, 1000 kW at the back wall

In this test the burner was moved from the centre of the floor to the back wall. The HRR was constant at 1000 kW during the test like in test A1. The PT temperatures on the wall (Figure 17) and in the ceiling (Figure 18) reached constant values faster compared to test A1.

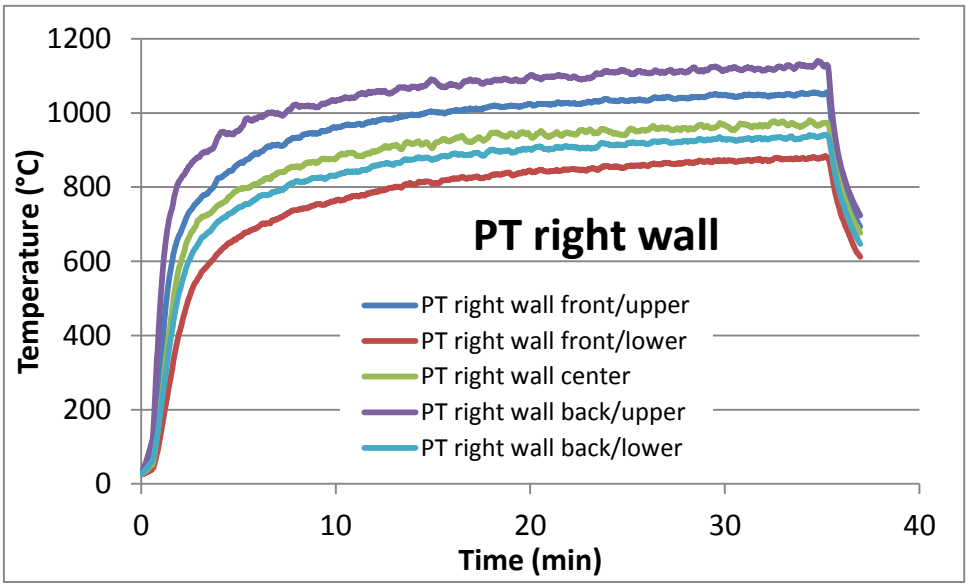

Figure 17. Test A3 - PT temperatures on the right wall.

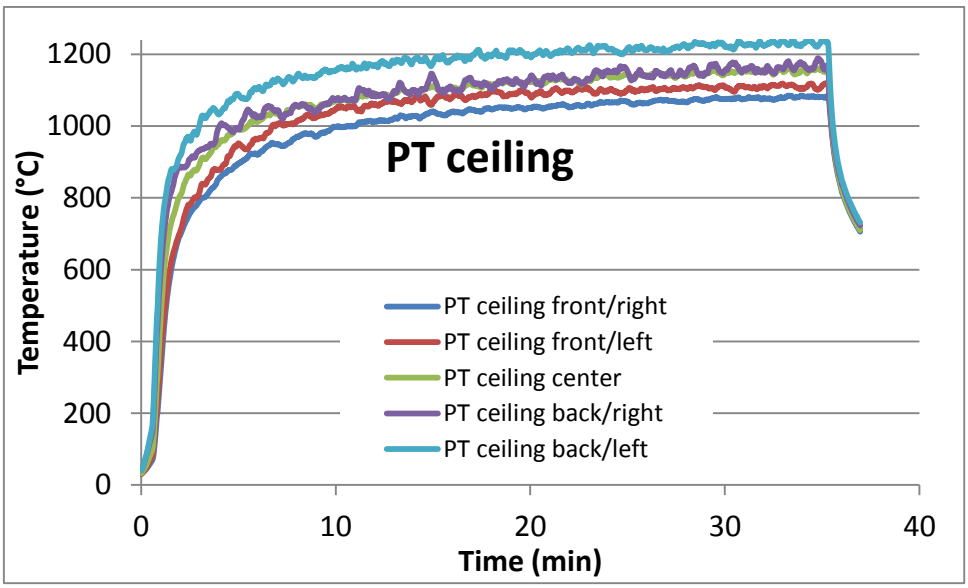

Figure 18. Test A3 - PT temperatures on the ceiling.

The TC tree temperatures in the opening stabilised long before the 35 minutes of fire exposure and the average after 30 minutes is shown in

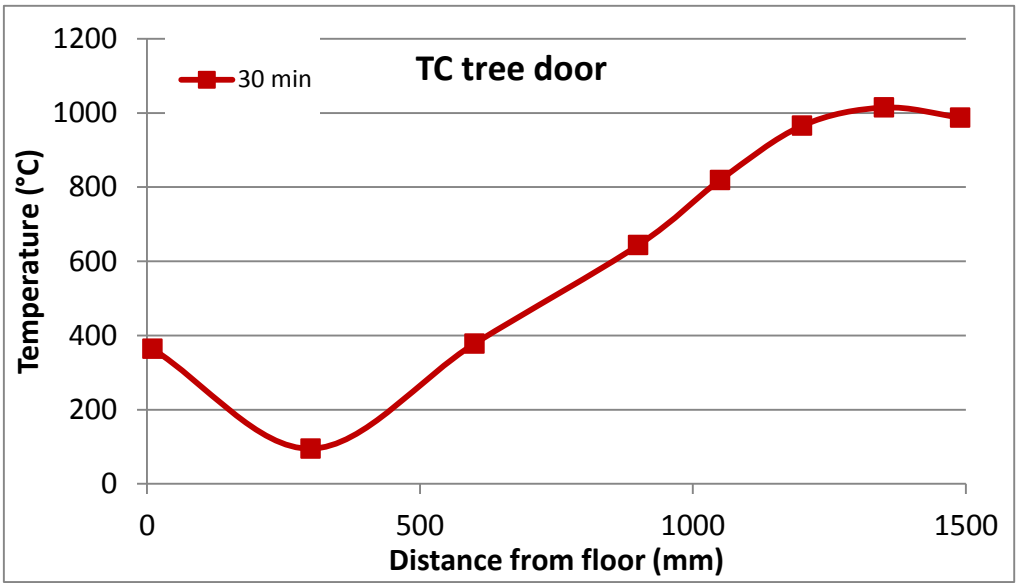

Figure 19. Test A3 – TC tree temperatures in the door opening during the test.

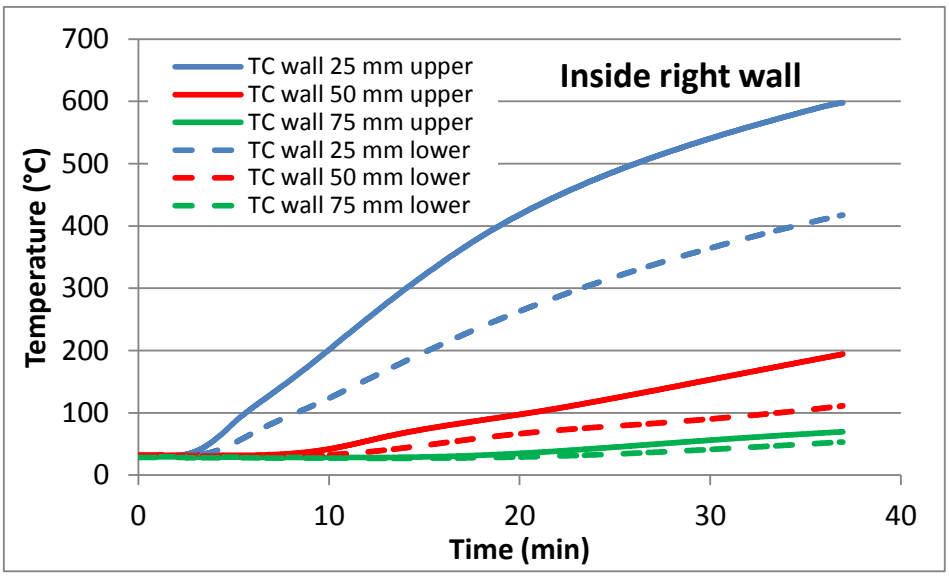

Figure 20. Test A3 - In-depth temperatures of the right wall at heights 1200 mm (upper – solid lines) and 600 mm (lower – dashed lines).

3.1.4 Test A4 - LWC, Ramp to 1250 kW

The burner was once again placed at the centre of the floor and the HRR was ramped from 250 to 1250 during 50 minutes and then kept constant at 1250 kW during 30 minutes. Figure 21 shows the HRR calculated from the calibrated flow of the propane burner.

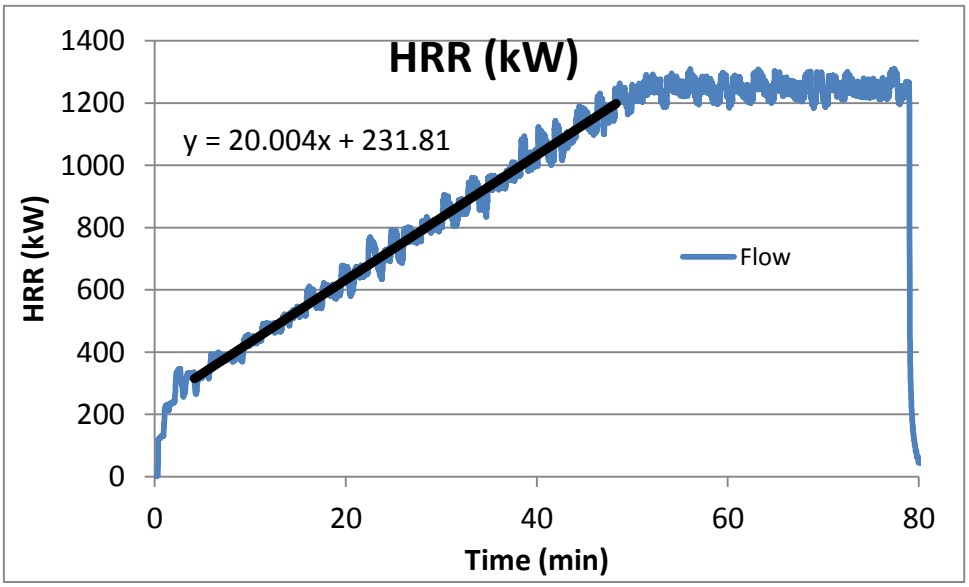

Figure 21. Test A4 - HRR calculated from the flow of the propane burner.

The PT temperatures on the right wall and in the ceiling established steady state conditions during the constant HRR phase, see figures below.

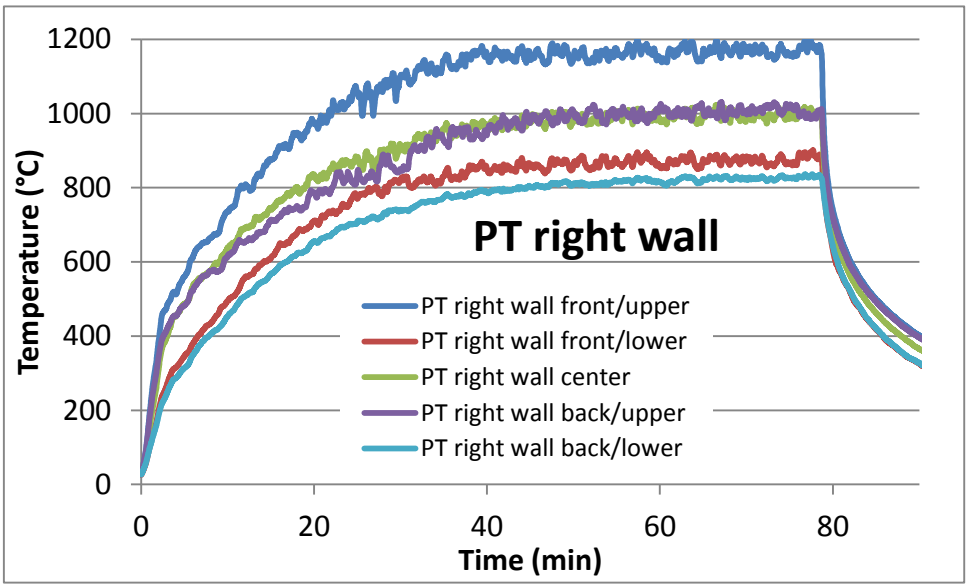

Figure 22. Test A4 - PT temperatures on the right wall.

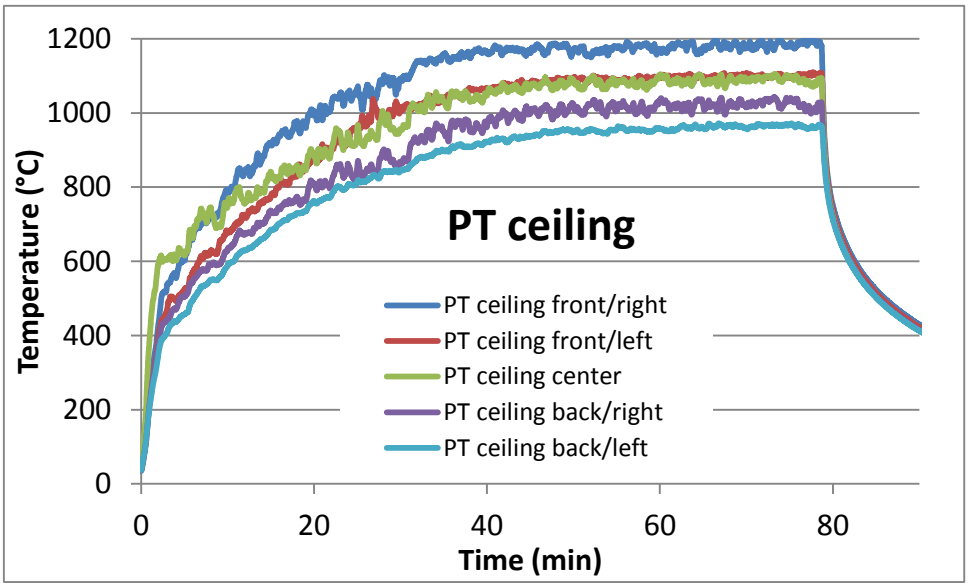

Figure 23. Test A4 - PT temperatures in the ceiling.

The equilibrium conditions of the TC in the opening are considered established after 60 minutes. Unfortunately the TC positioned at 1050 mm above floor level malfunctioned during the test, indicated by a gap in Figure 24.

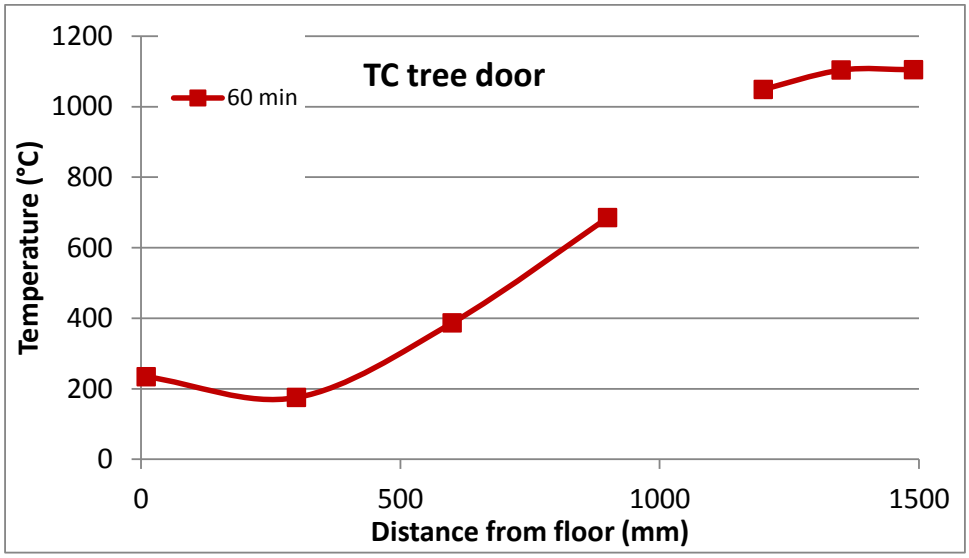

Figure 24. Test A4 – TC tree temperatures in the door opening during the test.

Very little effect of water in the walls can be noticed from test A4, Figure 25

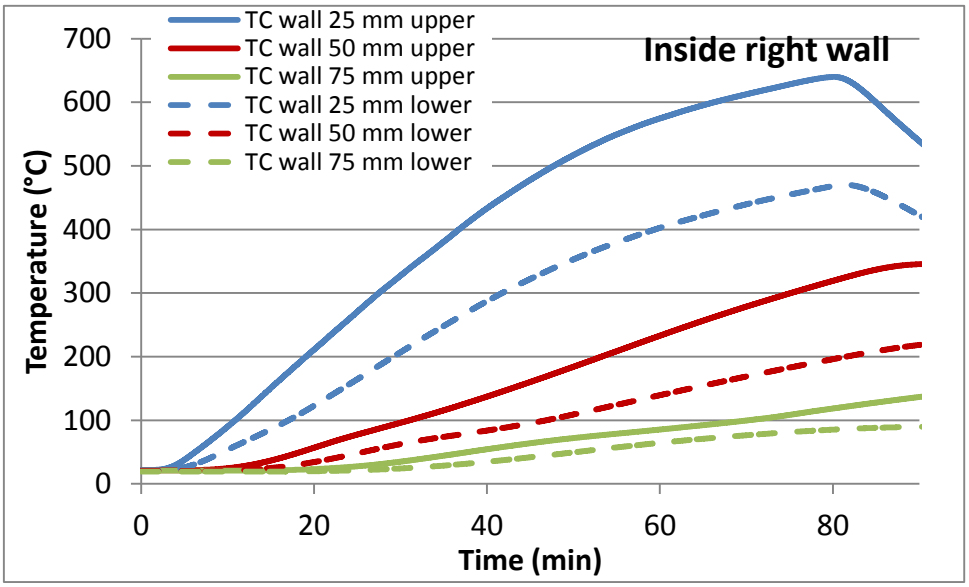

Figure 25. Test A4 - In-depth temperatures of the right wall at heights 1200 mm (upper – solid lines) and 600 mm (lower – dashed lines).

3.1.5 Test A5 – LWC, 1000 kW (repeat)

This test is identical to test A1 considering the HRR and placement of burner. The main difference lies in the fact that the moisture in the walls is mostly gone as this test starts. Figure 26 and Figure 27 shows higher temperatures of PT at wall and ceiling after one hour and a faster approach towards equilibrium.

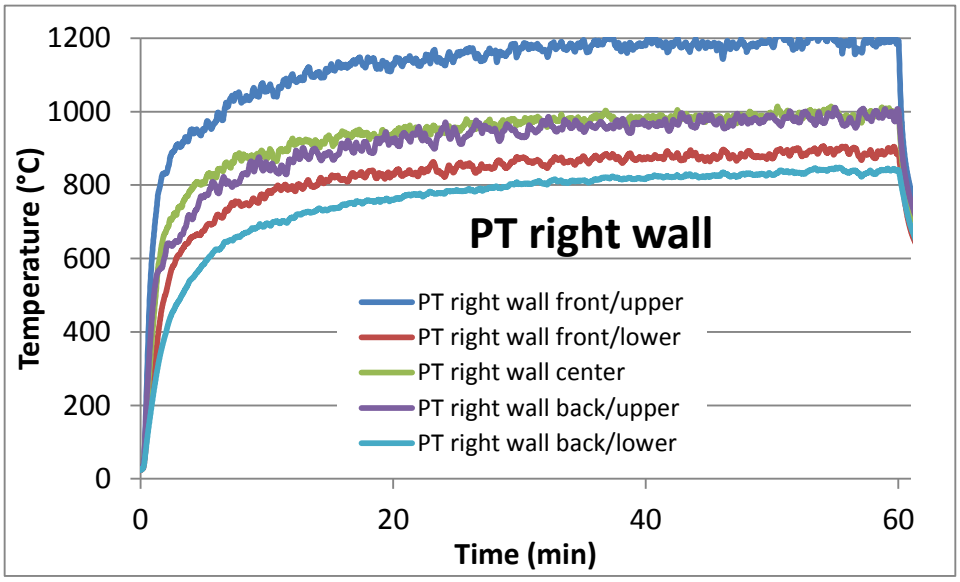

Figure 26. Test A5 - PT temperatures on the right wall.

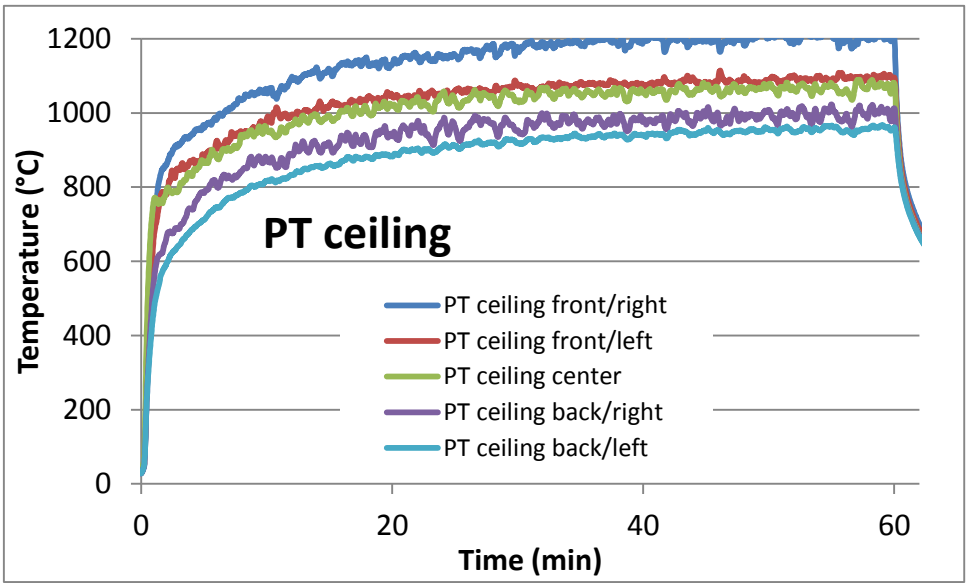

Figure 27. Test A5 - PT temperatures in the ceiling.

Once again the TC at 1050 mm height in the door opening malfunctioned but the inner TC tree was functioning, see Figure 28.

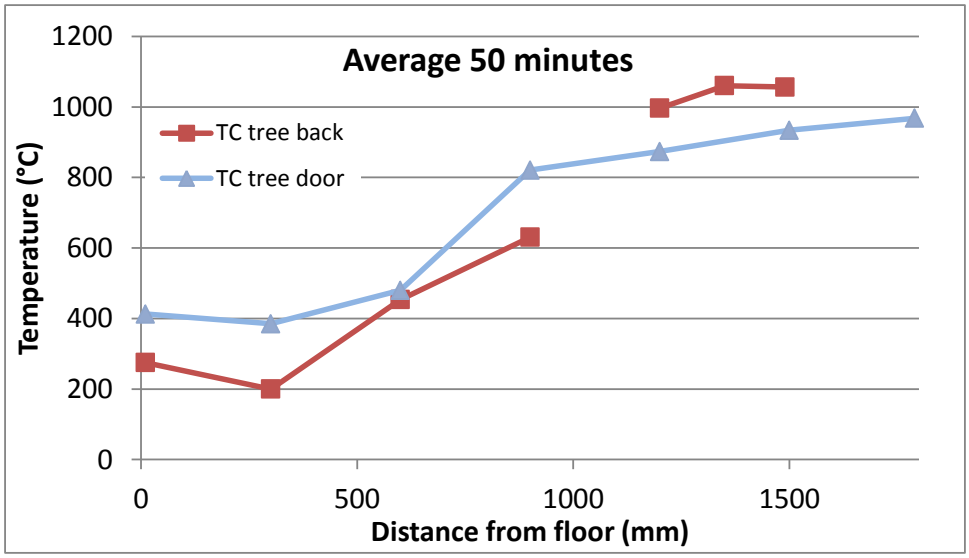

Figure 28. Test A5 – TC tree temperatures in the door opening and in the inner part of the enclosure (centrally positioned aligned with the opening and 675 mm from the back wall corresponding to 25 % of the full inner length, see Figure 4).

The moisture in the wall is not noticed from the Temperatures of the TC in the wall at this test, see Figure 29.

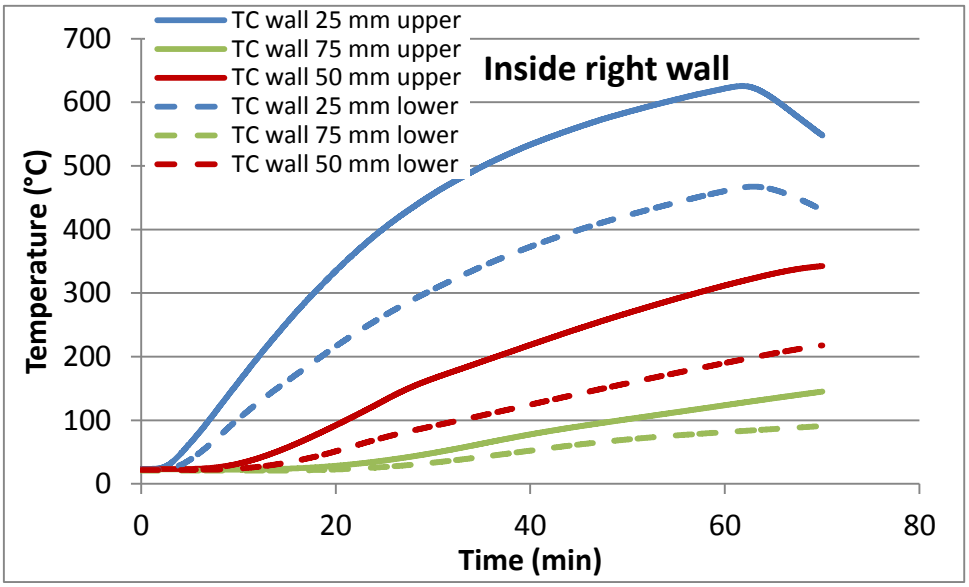

Figure 29. Test A5 – In-depth temperatures of the right wall at heights 1200 mm (upper – solid lines) and 600 mm (lower – dashed lines).

3.2 Test series B

This test series (as well as series C and D) were conducted in a larger burn hall compared to series A. This hall was equipped with an oxygen consumption calorimeter to measure the total HRR (the rate of energy released in the combustion) and the convective HRR (the rate of energy used to heat up the gases collected in the hood).

3.2.1 Test B1 – steel, insulated on inside – 1000 kW

The steel structure used in the remaining series was for series B insulated on the inside using stone wool with a nominal density of 200 kg/m^3 and a nominal thermal conductivity of 0.04 W/mK. The insulation thickness was 5 cm and therefore the enclosure inner dimensions were smaller in this series compared to all the other series. Figure 30 shows photos of the interior. The burner was placed in the centre and set at 1000 kW throughout the test. PT temperatures are shown from Figure 31 and Figure 32.

Figure 30. Photos of the interior surfaces of the test object before test B1.

Even in this test the recorded temperatures were not homogeneous but more severe on the right hand side.

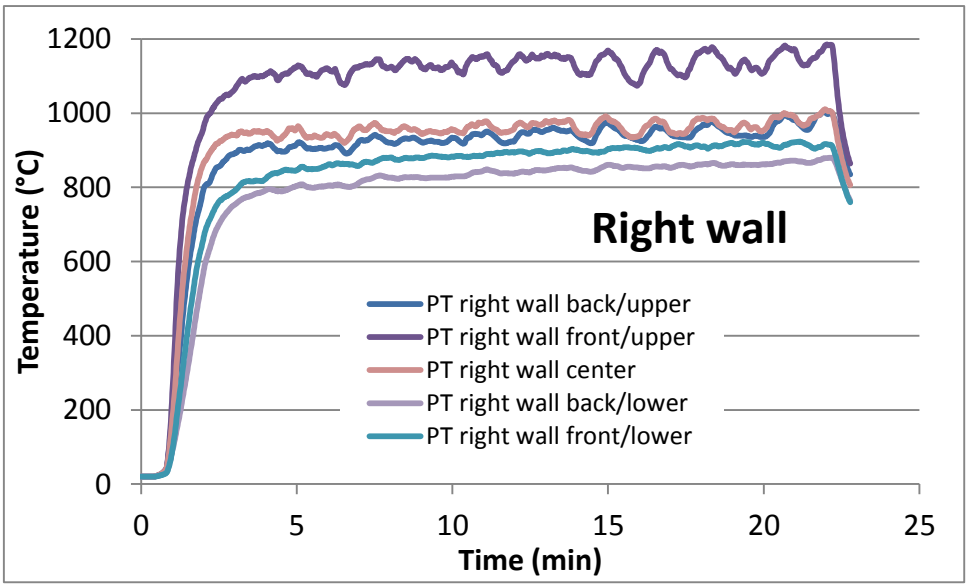

Figure 31. Test B1 –PT temperatures on the right wall.

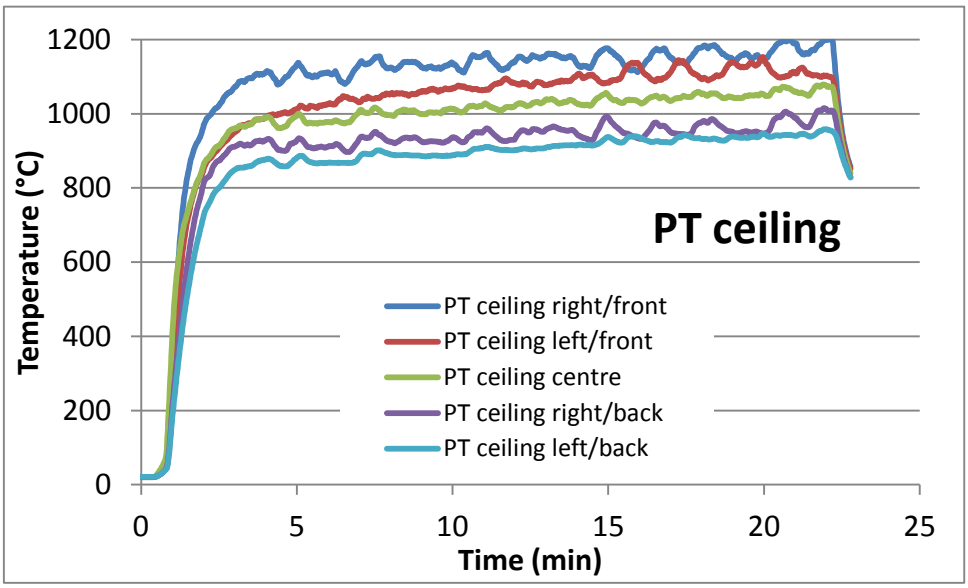

Figure 32. Test B1 –PT temperatures on in the ceiling.

As an example of how the insulation protects the steel Figure 33shows the steel temperature evolution throughout the test.

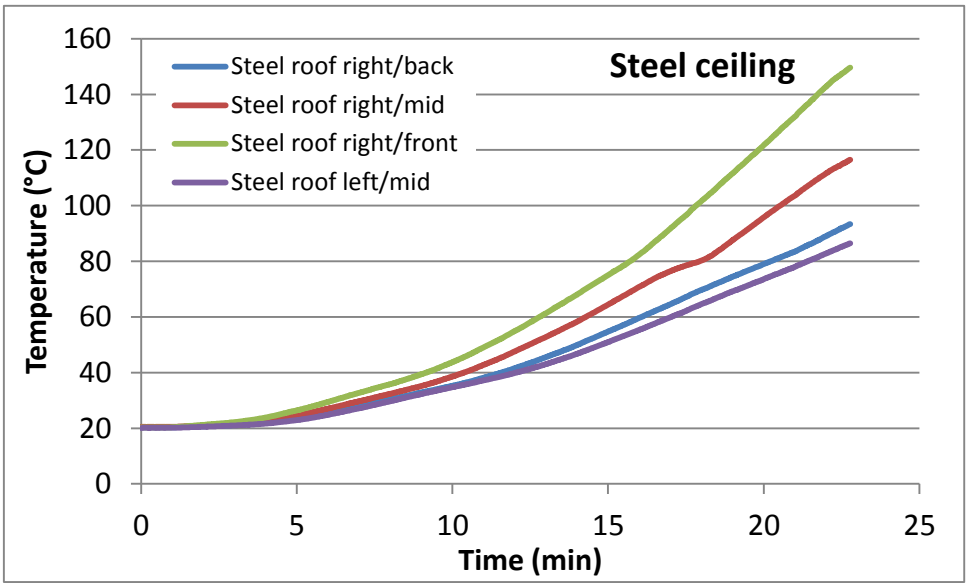

Figure 33. Test B1 - Steel temperatures in the ceiling. The positions are explained in Figure 6.

During the B1 test most TC tree thermocouples malfunctioned and no data is shown from this test.

Since an oxygen calorimeter was used in the B-D series the measurement of heat release rate was possible. Figure 34 shows the HRR of test B1 it is clear that the total HRR decreases during the test, an indication that the organic components of the mineral wool is burning.

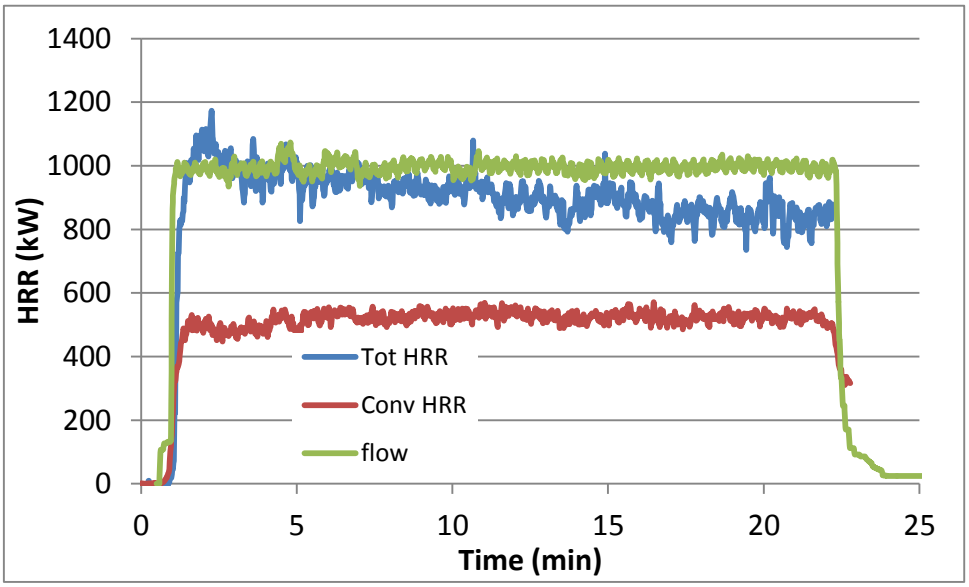

Figure 34. Test B1 – HRR measurement (blue, based on total consumption of oxygen), convective HRR (red, based on how much the gases have been heated) as well as the HRR based on the propane flow (green).

3.2.2 Test B2 – steel, insulated on inside – 1000 kW (repeat)

This test is identical to test B1 but the insulation is now already burned such that the exothermal combustion of binder and dust binding oil is absent in this test.

Figure 35. Photos from test B2.

PT temperatures of the right wall and ceiling are shown below.

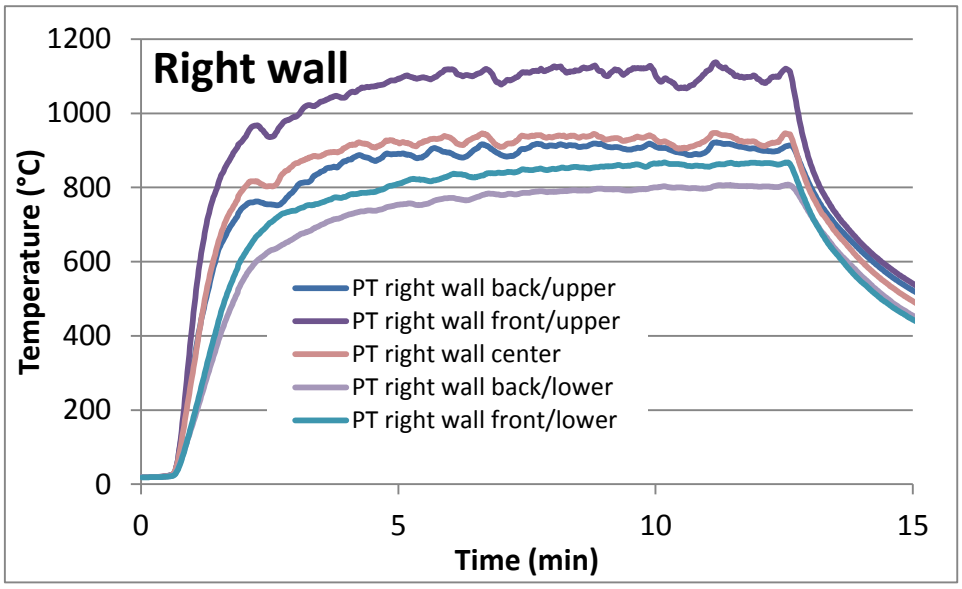

Figure 36. Test B2 –PT temperatures on the right wall.

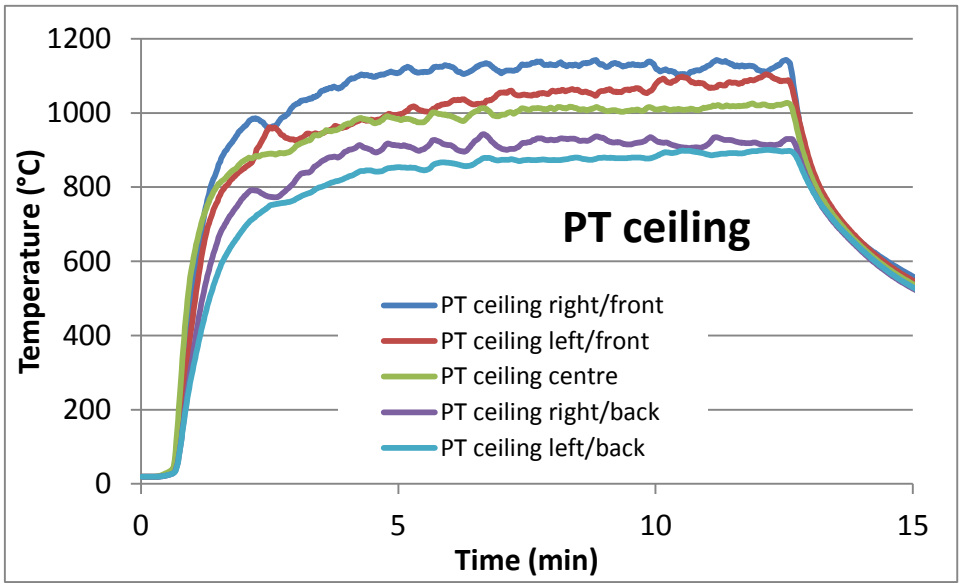

Figure 37. Test B2 –PT temperatures on in the ceiling.

After ten minutes all the temperatures (TC trees, and PT) in the compartment are considered constant. Therefore, the average temperatures from 10 to 12 minutes of the TC trees in the compartment and in the door opening are shown in Figure 38. It is notably warmer close to the floor in within the compartment. This is most likely due to the minimal convective cooling so close to the floor and therefore a larger dominance by radiant heating of TC, despite being only 1 mm thick and thereby very sensitive to convective heat transfer.

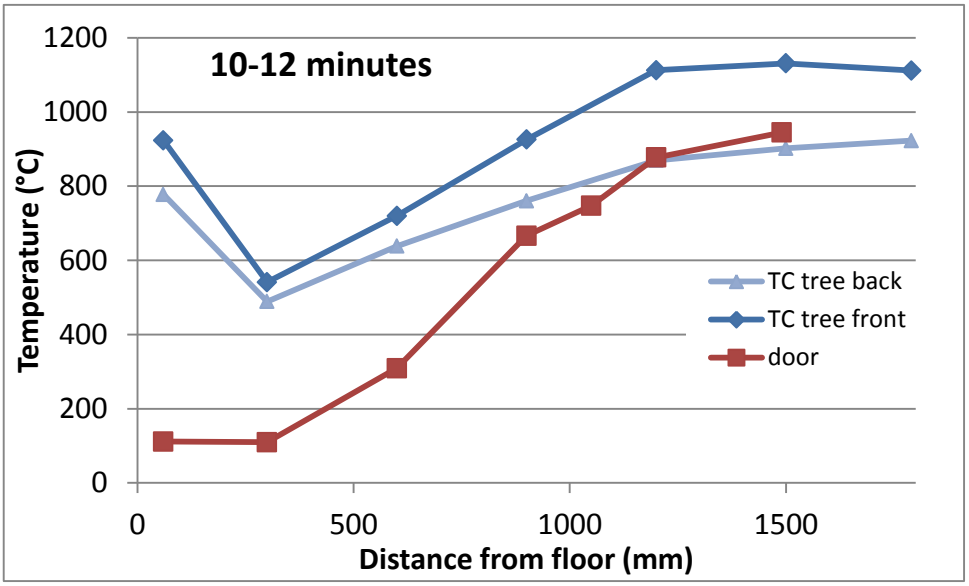

Figure 38. Test B2 –Steady state temperatures (average during 10-12 min) of the TC trees.

3.3 Test series C

The same 3 mm steel structure as test series B was used but all the insulation was. The inner dimensions were therefore exactly the same as series A (and D).

3.3.1 Test C1 – steel, uninsulated – 500 kW.

The HRR was set to 500 kW during the almost 30 minutes of exposure. No flames were visible outside of the opening of the enclosure. PT temperatures of wall and ceiling are shown in Figure 39 and Figure 40. For this low HRR the centre of the ceiling is the hottest.

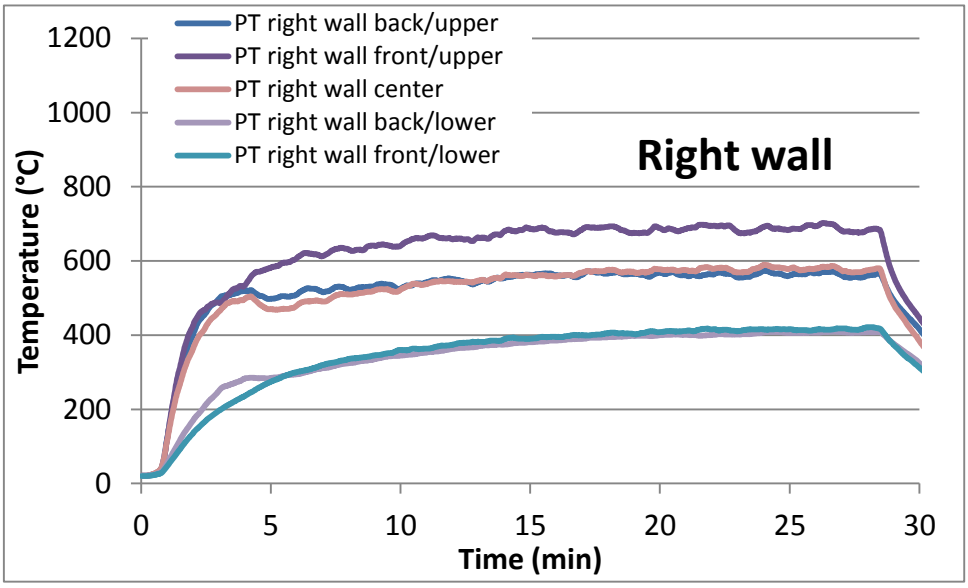

Figure 39. Test C1 –PT temperatures on the right wall.

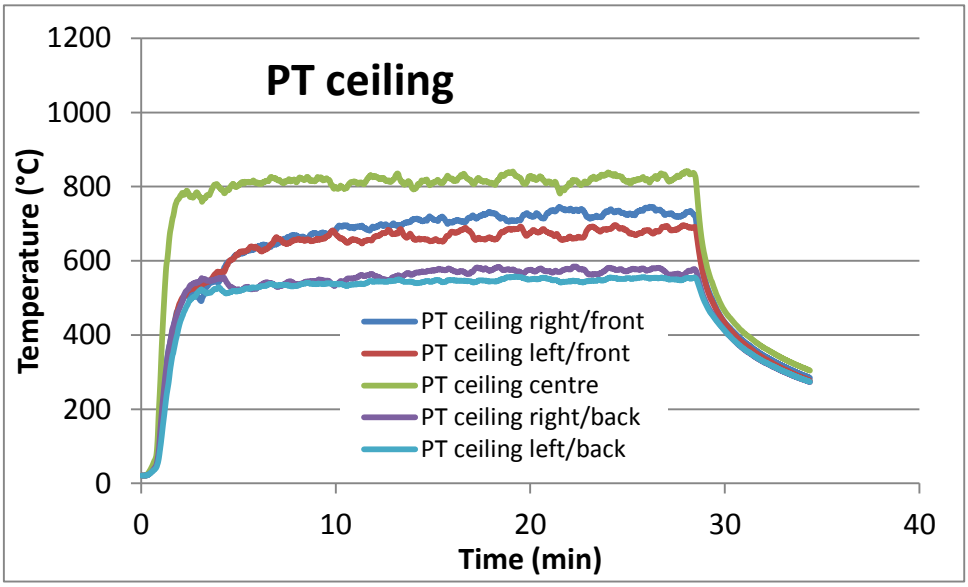

Figure 40. Test C1 –PT temperatures on in the ceiling.

The TC tree temperatures are considered stable after 25 minutes and we define the steady state temperatures as the average over 25-27 minutes.

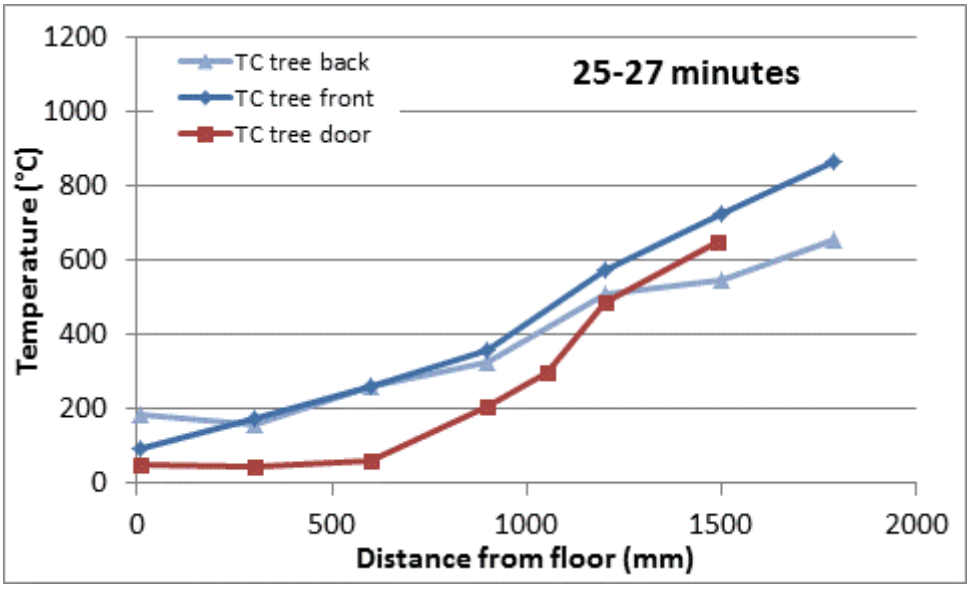

Figure 41. Test C1 –TC tree temperatures in steady state conditions (averaged over 25-27 minutes).

The steel temperature evolution is shown in Figure 42.

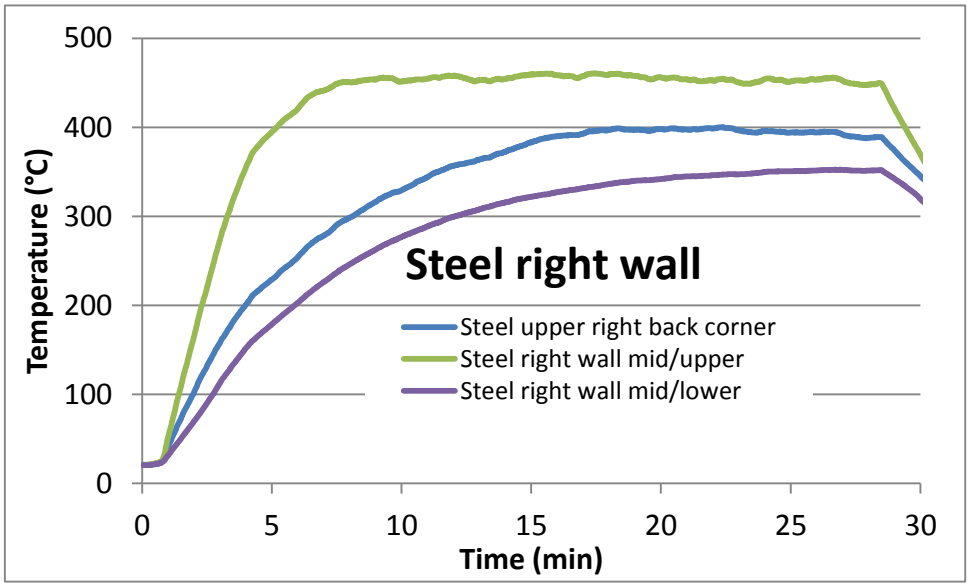

Figure 42. Test C1 –Steel temperatures of the right wall.

3.3.2 Test C2 – steel, uninsulated – 1000 kW

As the burner was constant at 1000 kW there were much flames reaching out of the opening, unlike for the 500 kW C1 test but similar to 1000 kW tests in series A and B. Temperatures of the PT are shown in Figure 43 and Figure 44.

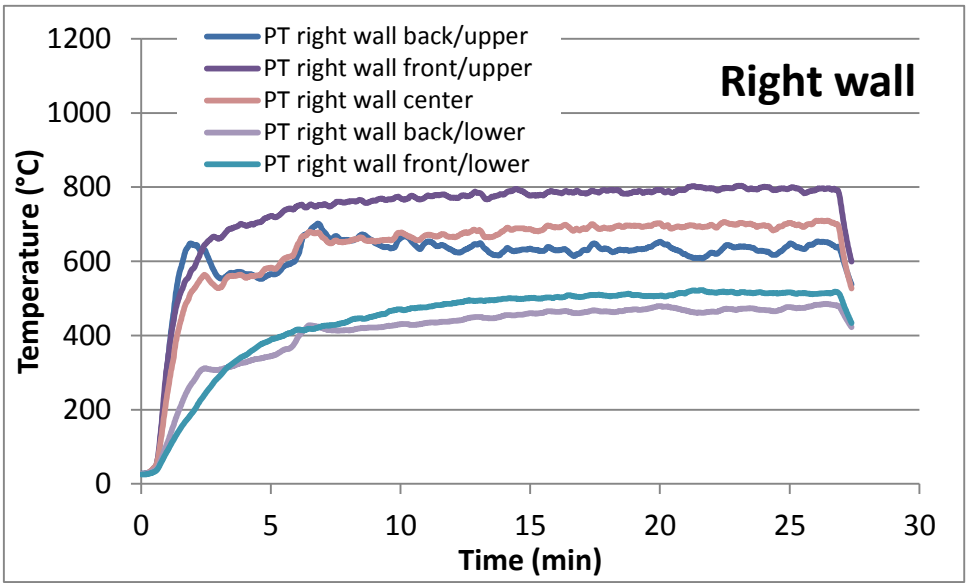

Figure 43. Test C2 –PT temperatures on the right wall.

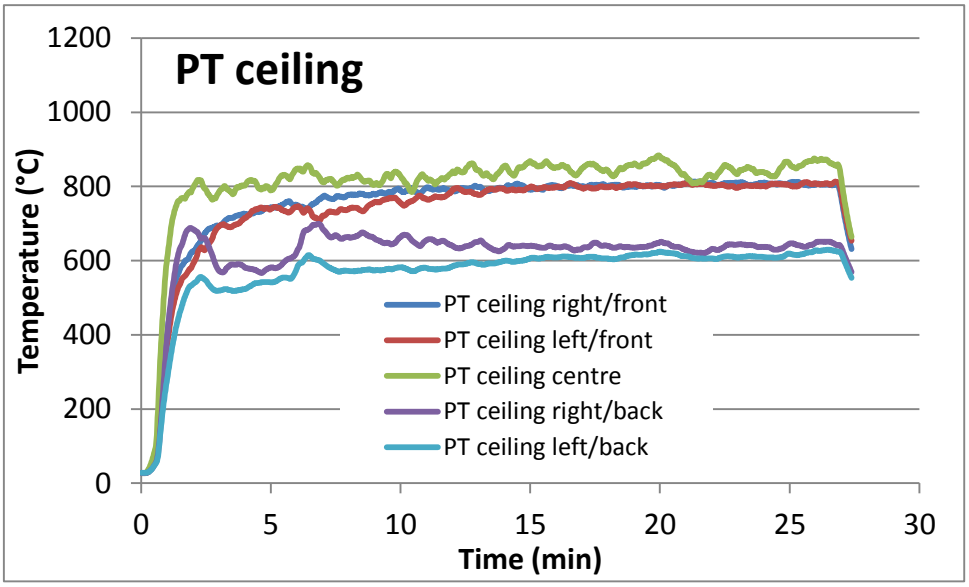

Figure 44. Test C2 –PT temperatures on in the ceiling.

Between 20 and 25 minutes the TC tree temperatures are considered constant within the usual fluctuations and the average during that time is considered the steady state TC tree temperatures, shown in Figure 45

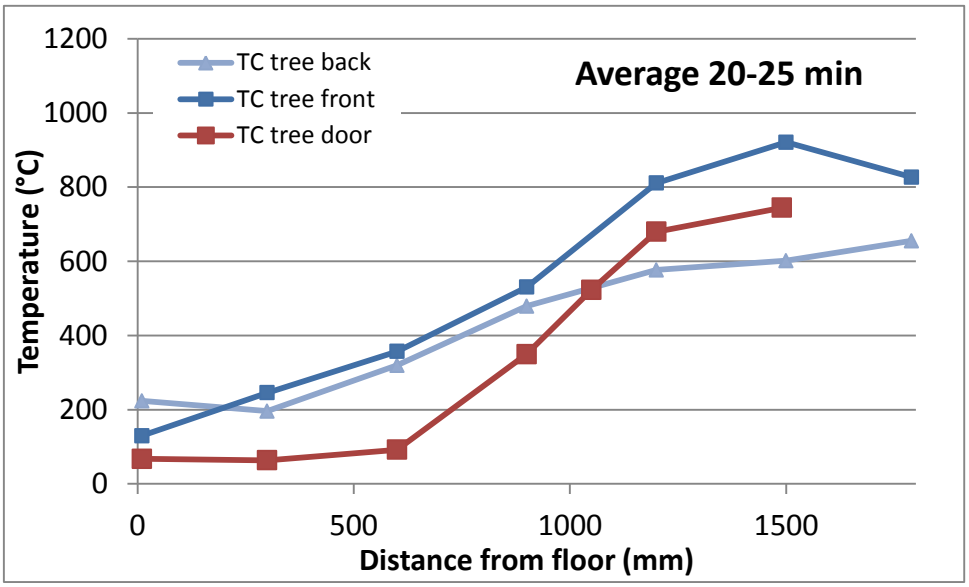

Figure 45. Test C2 –TC tree temperatures during steady state conditions.

3.3.3 Test C3 – steel, uninsulated – Ramp to 1250 kW

This test used the ramping fire starting at 200 kW, increasing at 60 kW per minute and constant at 1250 kW after 17.5 minutes, see Table 1. Figure 46 shows the measured HRR based on the propane mass flow, and measured by the oxygen consumption calorimeter in the burn hall. Three photos of the door opening for different HRR are shown in Figure 47.

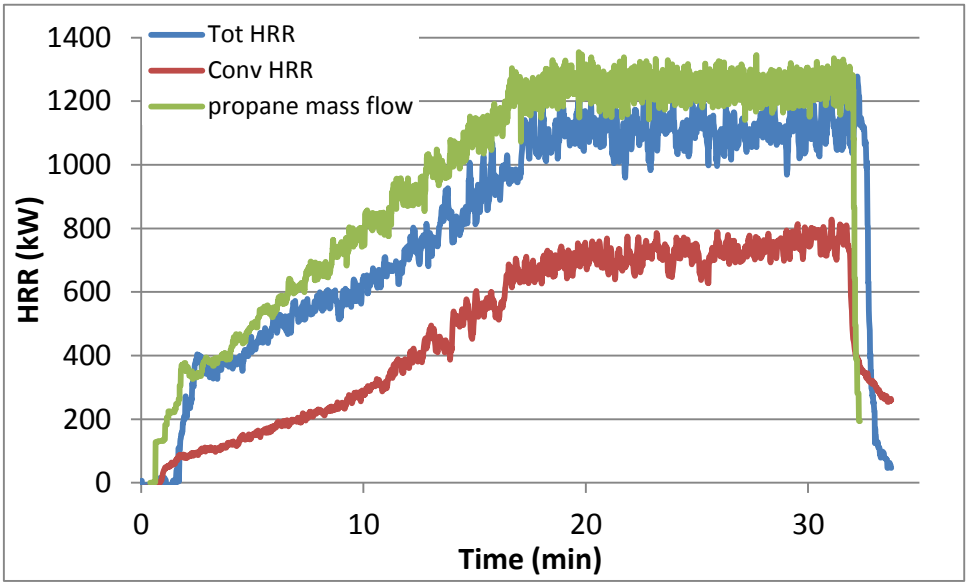

Figure 46. Heat release rates from test C3.

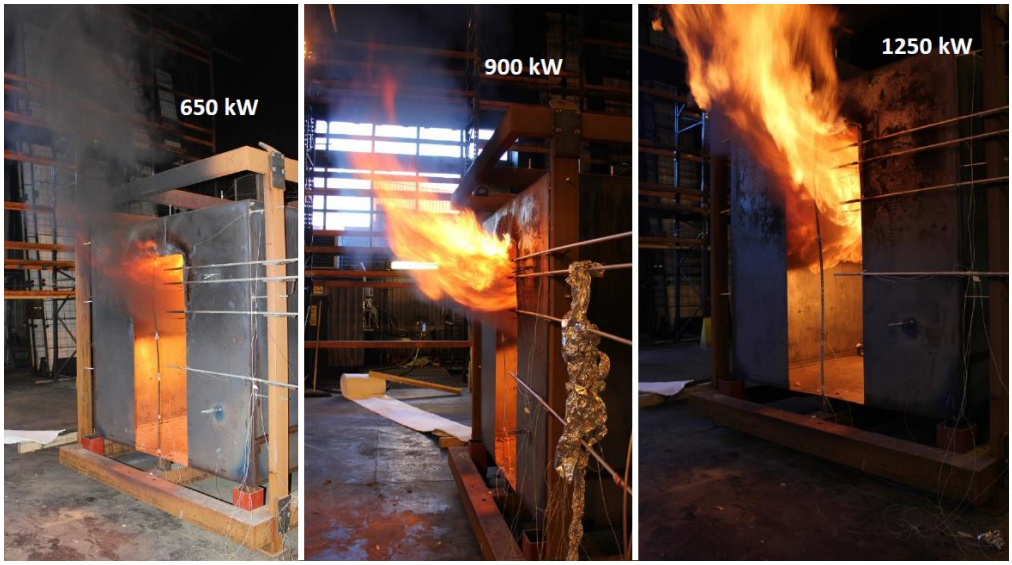

Figure 47. Photos from test C3 at different heat release rates (as defined by the gas flow).

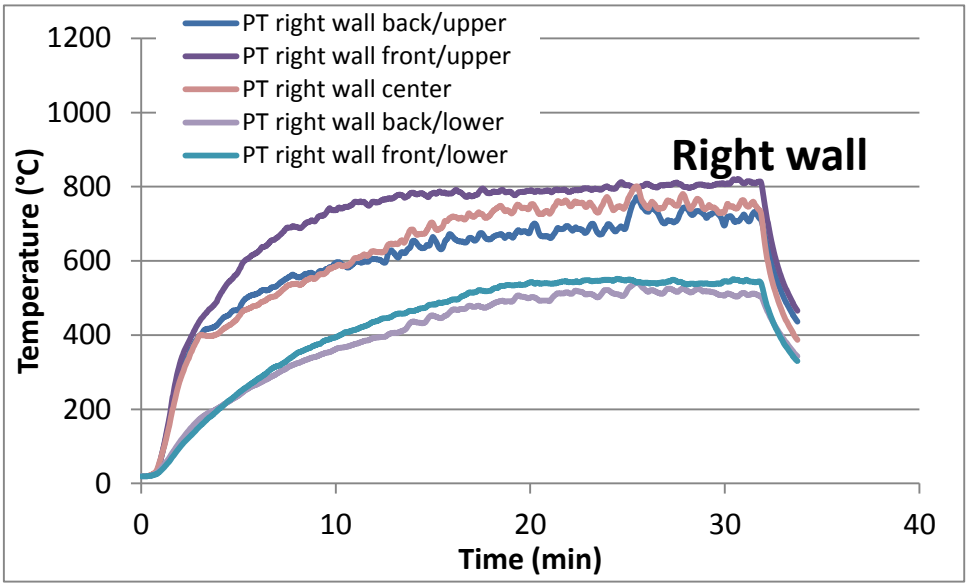

Figure 48. Test C3 –PT temperatures on the right wall.

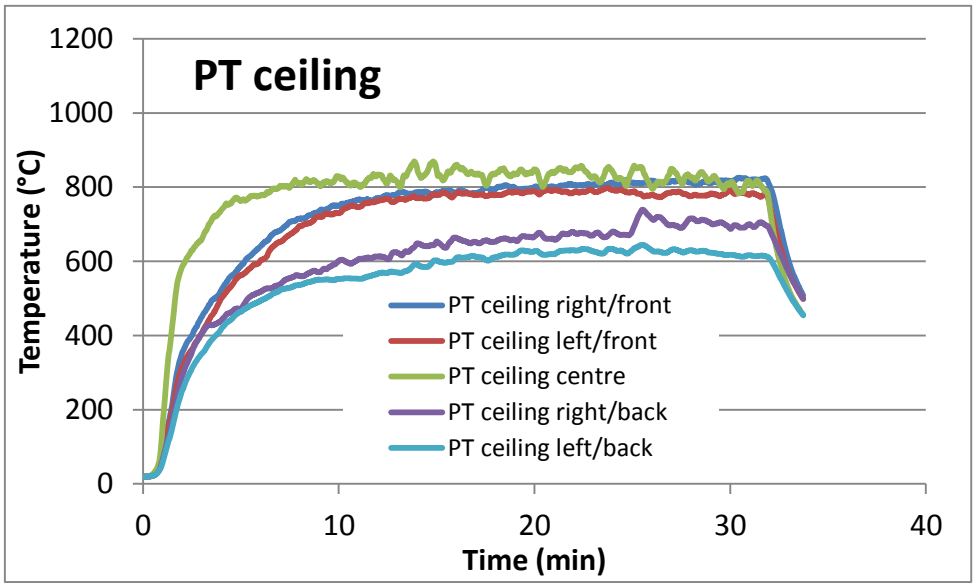

Figure 49. Test C3 –PT temperatures in the ceiling.

Between 27 and 30 minutes steady state is considered reached for the TC tree temperatures, see Figure 50.

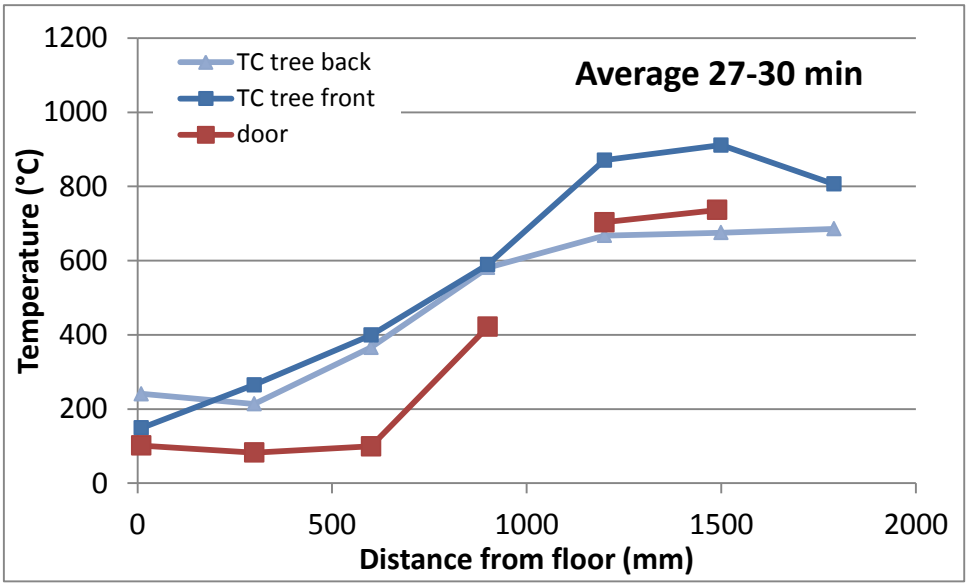

Figure 50. Test C3 –TC tree temperatures during steady state (average over 27 and 30 minutes). The TC at 1050 mm malfunctioned during the test.

Temperatures of the steel in the right wall is shown in Figure 51.

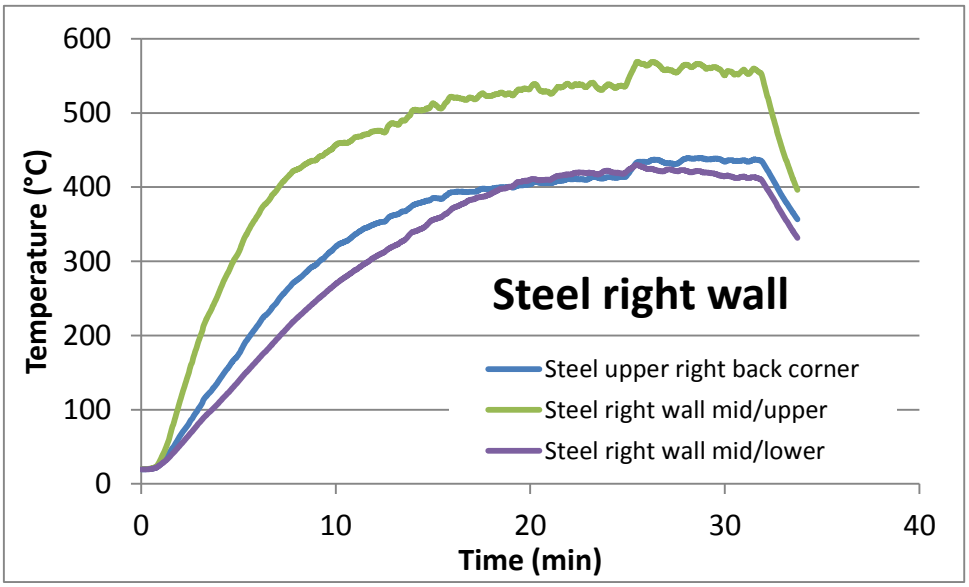

Figure 51. Test C3 –Steel temperatures of the right wall.

3.4 Test series D

The steel structure was insulated from the outside with 50 mm stonewool of nominal density 200 kg/m^3 on all six surfaces. Two tests with identical propane mass flow levels (1000 kW) were performed.

3.4.1 Test D1 – steel, insulated outside – 1000 kW

During the almost 35 minutes that the test lasted the not all PT reached equilibrium conditions. However, considerably higher temperatures compared the 125 kW C3 test was reached. PT temperatures of right wall and ceiling are shown in Figure 52 and Figure 53, respectively.

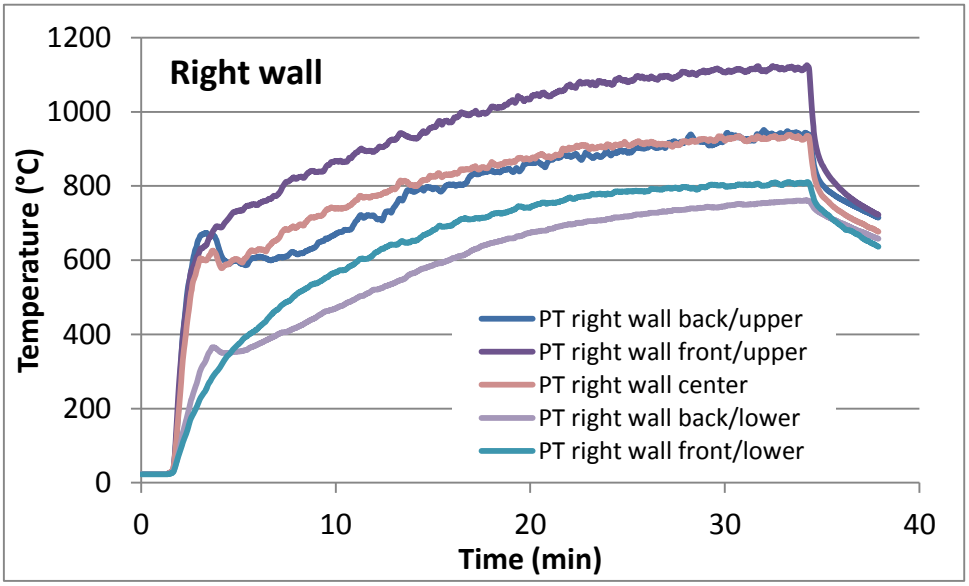

Figure 52. Test D1 – PT temperatures on the right wall.

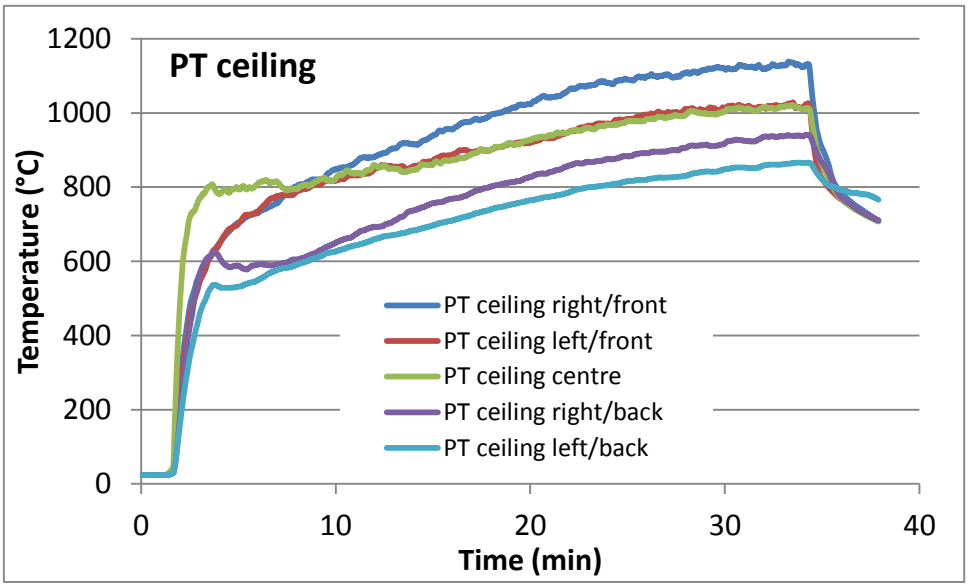

Figure 53. Test D1 – PT temperatures in the ceiling.

The temperatures of the TC trees had not completely established steady state at the end of the test but the increasing trend was very weak and the 30-34 minutes average is considered as an acceptable representation of equilibrium conditions, see the data spreadsheet for the temperature evolution of the TC trees. Figure 54 shows the temperatures at the three different positions.

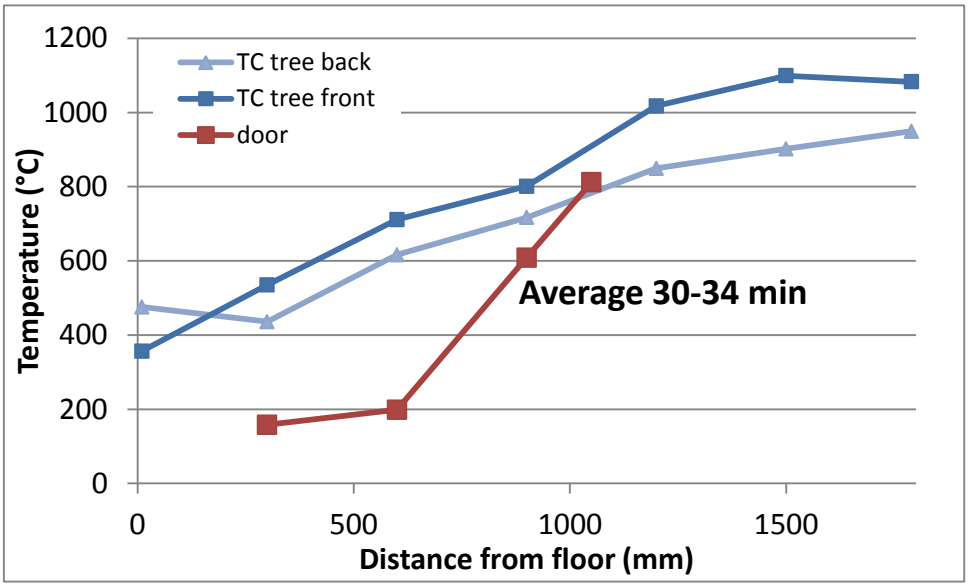

Figure 54. Test D1 – TC tree temperatures. Only four of the door opening TC functioned during the test.

The steel temperatures of the right wall is shown below.

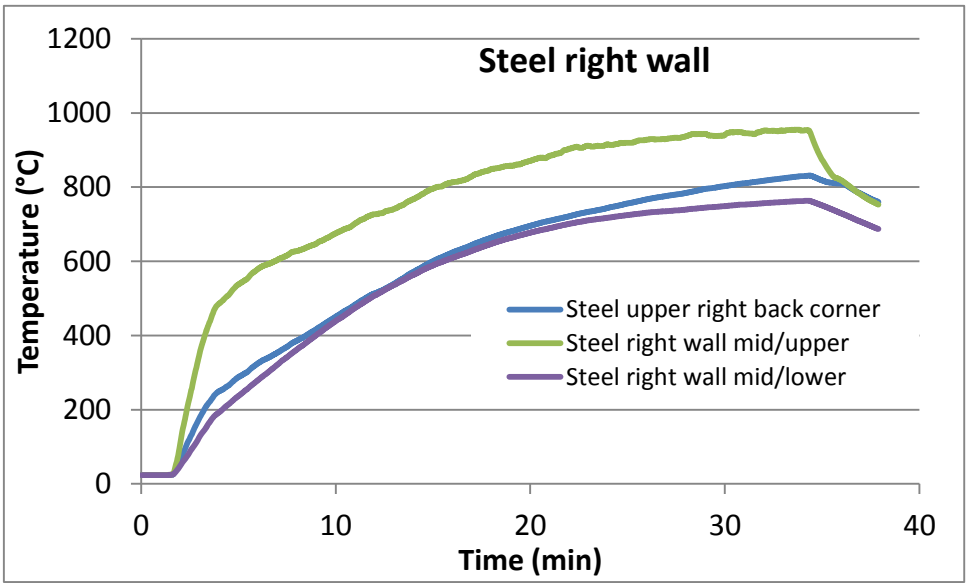

Figure 55. Test D1 – Steel temperatures of the right wall.

3.4.2 Test D2 – steel, insulated outside – 1000 kW (repeat)

The same test as test D1 was performed. The only difference was that the external stonewool had already been hot once. The recorded final gas and steel temperatures are very similar and Figure 56 shows PT temperatures of the right wall where the comparison to Figure 52 can be made. The only difference between the tests are in the first minutes where the temperatures of the steel increases faster in the second (D2) test, see Figure 57.

No more data from this test is shown here due to the similarity with test D1 but all data is available in the spreadsheet data.

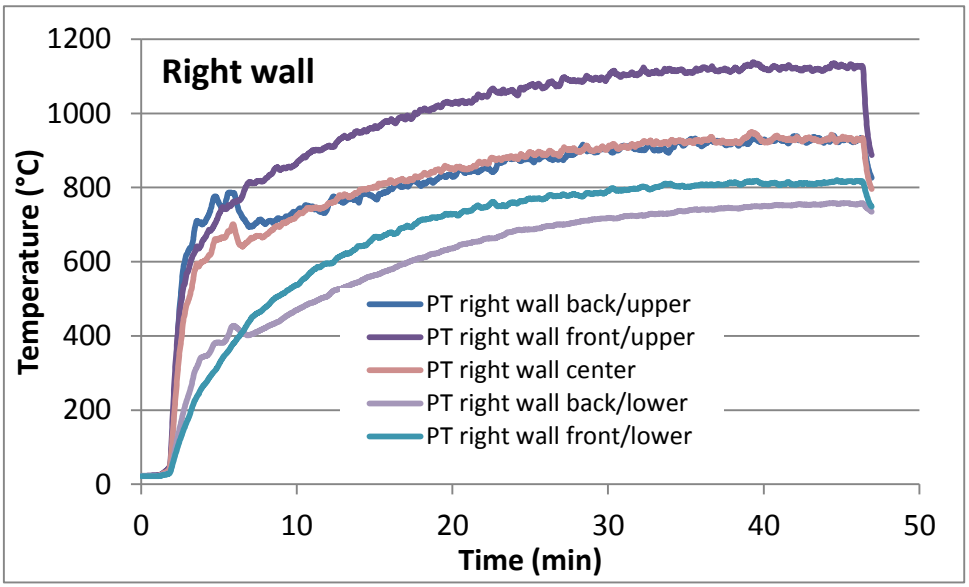

Figure 56. Test D2 – PT temperatures of the right wall.

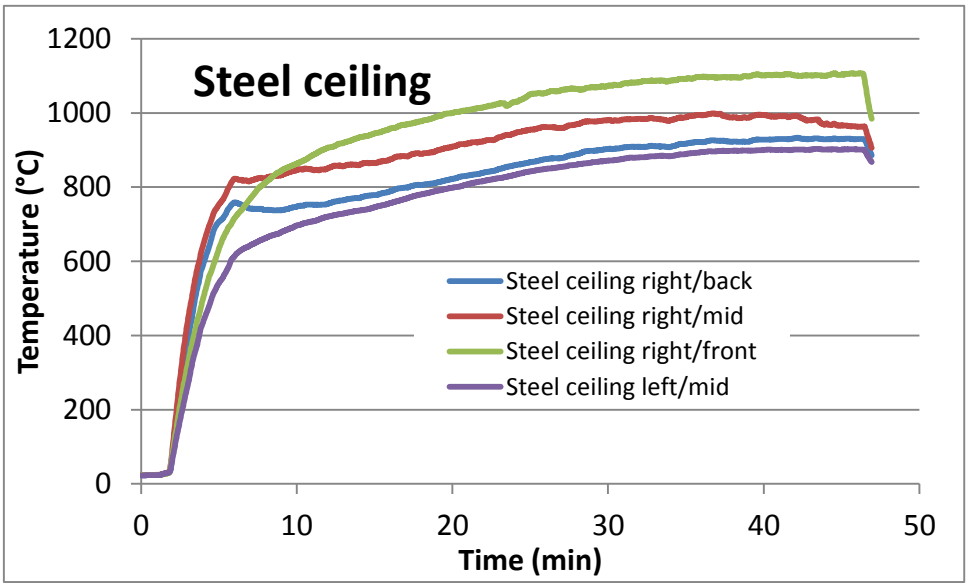

Figure 57. Test D2 – Steel temperatures in the ceiling.

4 Discussion

This chapter briefly describes some differences between the results from tests. It is by no means a conclusive analysis but it highlights the effects of various conditions and identifies some interesting features.

4.1 Effects of different wall materials

Below comparisons are made between the tests with a burner output of 1000 kW in enclosures with different enclosure structures. Approximately the same final temperatures are reached in the insulated cases (A5 – LWC, B2 – steel with insulation inside and D2 – steel with insulation outside). However, the time it takes to reach the final temperature is very different. Two examples are shown in Figure 58 (PT right wall front/upper) and Figure 59 (TC tree at 1200 mm height in door opening).

The high density in the LWC case yields a long time for equilibrium conditions whereas the B-series, insulation inside the enclosure reaches final temperatures after only a few minutes. When the insulation is outside the steel, the fire temperature rise rate is significantly reduced due to the direct exposure of the heat sink of the steel. However, notice that the final temperature is the same. With uninsulated steel the final temperature is several hundred degrees lower than in the other cases.

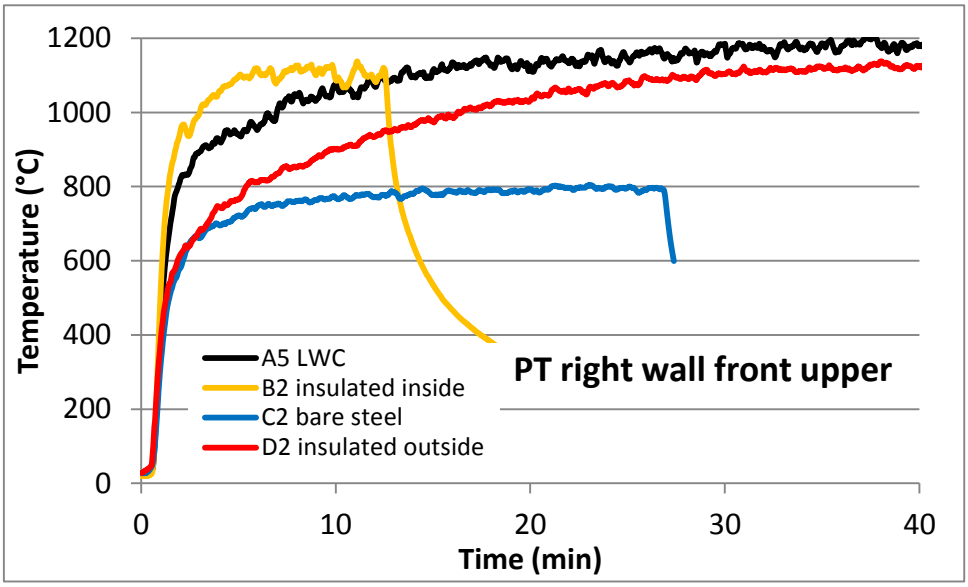

Figure 58. Comparison of the PT temperatures on the right wall in the front/upper position in the tests with 1000 kW for different surrounding structures.

Note also that steady state conditions are approached faster in the ceiling, where fire exposure is more severe compared to the wall. This is evident by comparing e.g. Figure 43 and Figure 44.

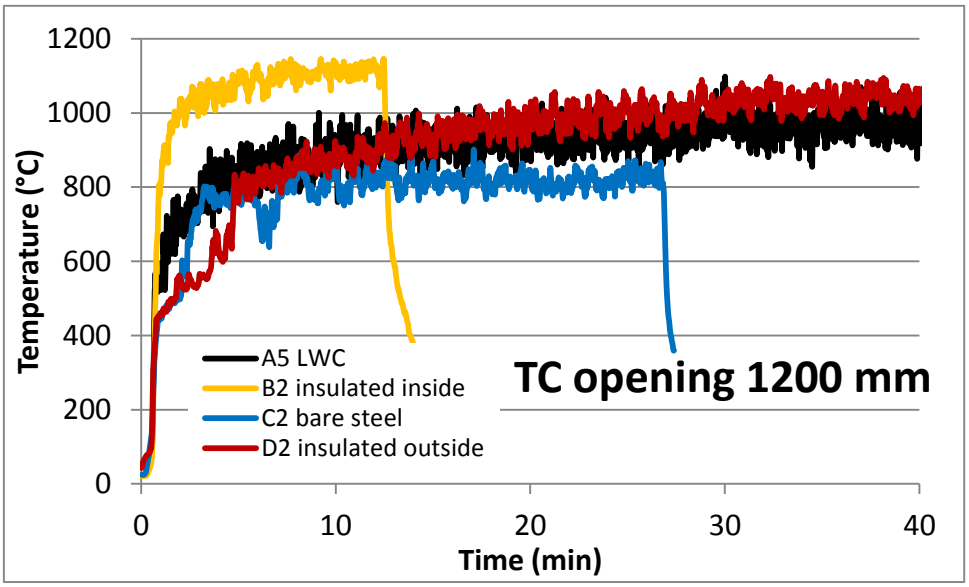

Figure 59. Comparison of the temperatures of TC 1200 mm from floor in the tests with 1000 kW for different surrounding structures.

4.2 Effect of moisture in LWC surrounding structures

Test A1 and A5 are identical except that the moisture in the wall is mostly absent in test A5. Figure 29 shows that there are very some effects of moisture evaporation at 75 mm depth in test A4, indicating that free water is not affecting test A5. The water present in test A1 is not only affecting the temperatures within the wall but also, to a large extent, the fire temperatures measured with PTs. It is evident from Figure 60, both in the short time response and the asymptotic behaviour (almost 100 °C difference after one hour of exposure), even though the water eventually would evaporate and the two tests would finally reach the same temperatures.

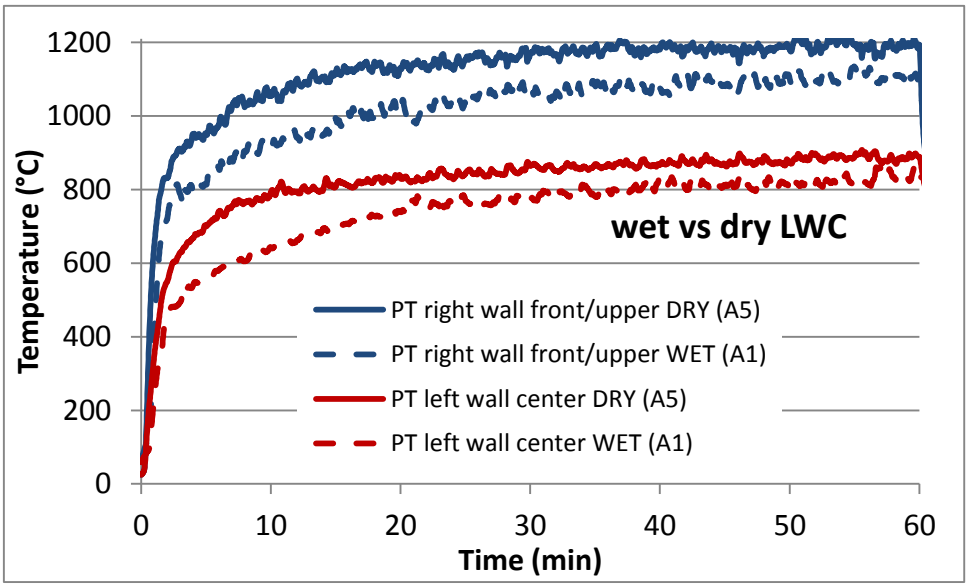

Figure 60. PT temperature in the LWC structure with 1000 kW HRR. The effect of walls containing free water and not.

However, for the gas temperatures in the upper part of the door opening, the main difference is in the early stage while no large effects of the LWC moisture are seen later on, see Figure 61.

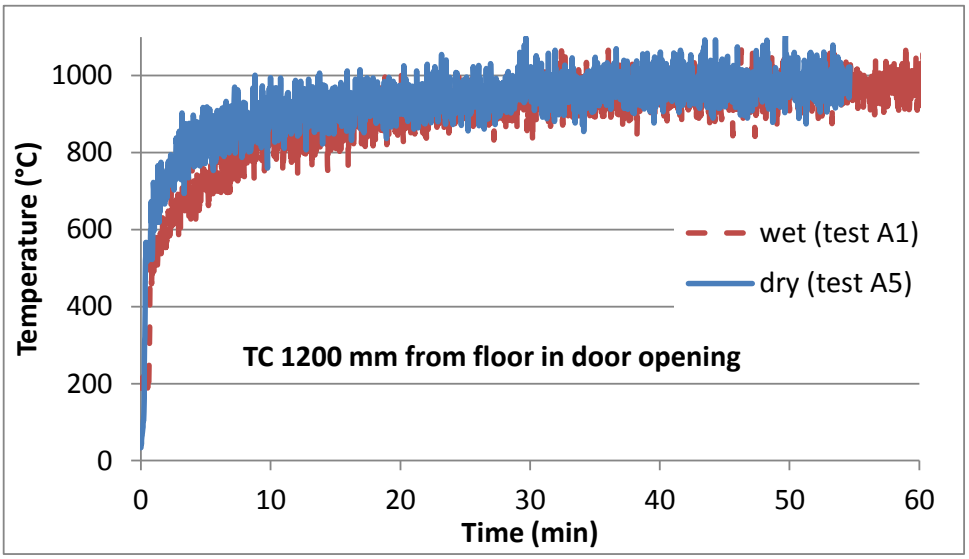

Figure 61. TC temperature in door opening, 1200 mm from the floor in the LWC structure with 1000 kW.

4.2 Effect of burner placement

Test A3 and A5 are identical except that the burner placement is on the back wall in test 3 and in the centre in test A5. We notice that the effects of moisture are low in test A3 (Figure 20). Therefore, test A5 is a suitable comparison to test A3. Naturally the burner placement creates local variations such as a higher temperature at the back wall when burner is placed there but the effect on the front wall or in the gas temperatures in the opening is negligible as seen in Figure 62. A somewhat faster heating is noticed for the case when the burner is in the centre. This is most probably due to a larger absorption of heat at the back wall in test A3. After the initial fast heating, the gas temperature and thermal exposure to the front wall become close to identical regardless of the burner placement.

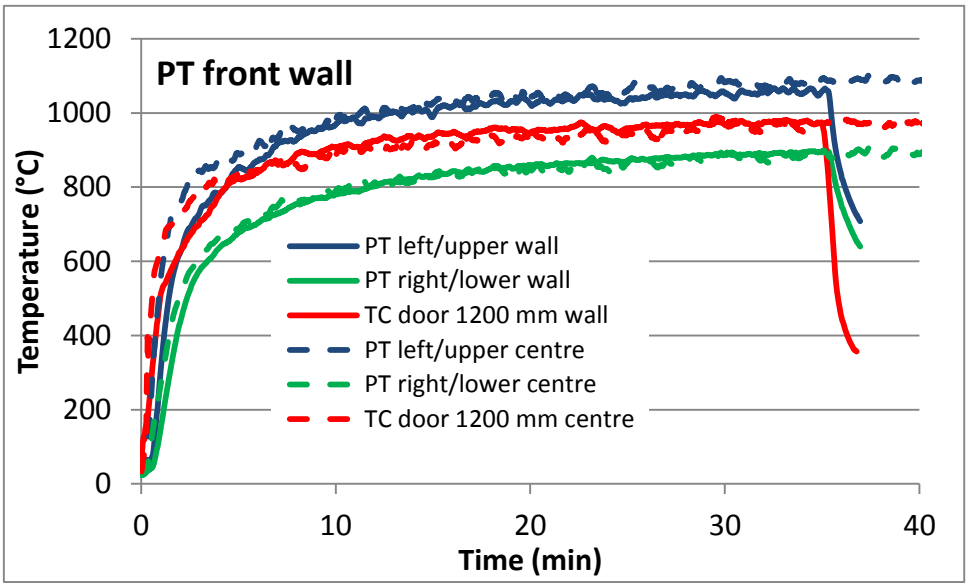

Figure 62. Comparisons of PT temperatures at the front wall and TC temperatures in the opening between test A3, burner at back wall (solid lines) and A5, burner at centre (dashed lines).

4.3 Effects of insulating the steel

Test C2 and D2 differ in that insulation is added on the outside for test D2. The difference between the two tests is very big as can be seen in Figure 63 showing the steel temperatures of the ceiling (right/front) as well as the TC temperatures at 1200 mm height in the opening. The ceiling temperature in the uninsulated case reaches rapidly its final temperature of 600 °C while for the insulated structure the increase is much slower as the heat slowly penetrates the insulation. The difference in temperature between insulated and uninsulated steel after 30 minutes would have been 500 °C and rising (if test C2 would have continued for that period).

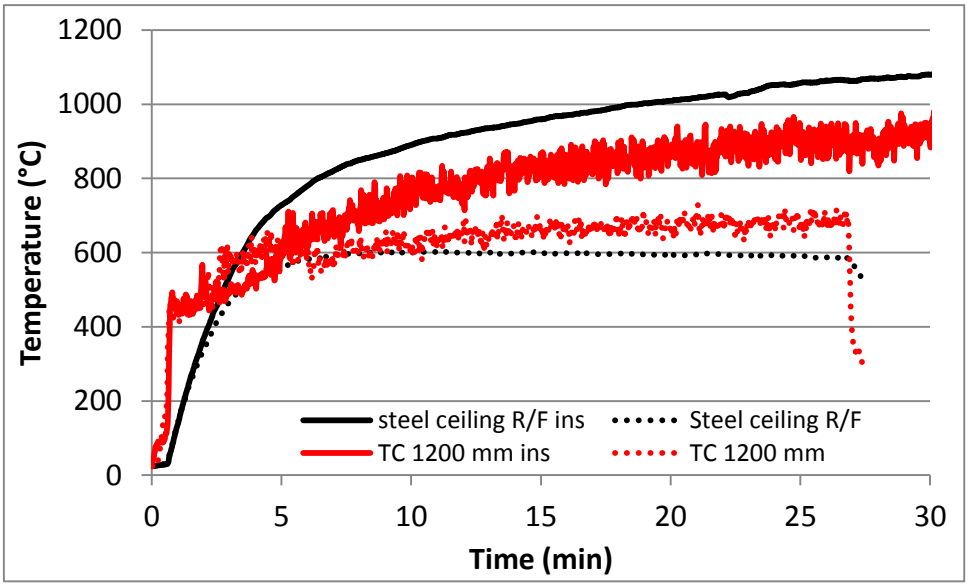

Figure 63. Comparison of steel temperatures in the ceiling (black solid line for insulated steel and black dotted line for bare steel) and TC temperatures in the opening at height 1200 mm (red solid line for insulated steel and red dotted line for bare steel. R/F denotes the right/front position. Test D2 is shifted in time to match test C2 to the same ignition time.

4.4 Effects of combustible binder content in mineral wool

Combustible products (binder) in the mineral wool will burn and contribute to the HRR of the compartment as well as to a temperature rise in the structure and consequently in the fire compartment. Comparing test B1 and B2 the flow of propane is identical but the measured HRR differs, being markedly larger in test B1, in which most of the combustion of binder and dust binding oil of the mineral wool takes place. Figure 64 shows the comparison of the two tests. Integrating the measured HRR curves from 0 to 13 minutes yields a net difference between the two tests of 65 MJ. The volume of the mineral wool is 1.12 m^3. Assuming 4 % combustible material yields almost nine kg of binder and dust binding oil which approximately would produce 120 MJ on complete combustion (given 14 MJ/kg heat of combustion (Sjöström & Jansson, 2012)). The large difference between the approximately calculated value and the measured value is explained with the fact that the heat does not penetrate the complete mineral wool value to such an extent that the oils of the insulation undergo combustion throughout the whole thickness during the twelve minutes of exposure for both tests. The HRR of test B1 is still clearly decreasing after 13 minutes and if integration would have been possible to a longer burn time the difference in THR would probably be closer to 120 MJ.

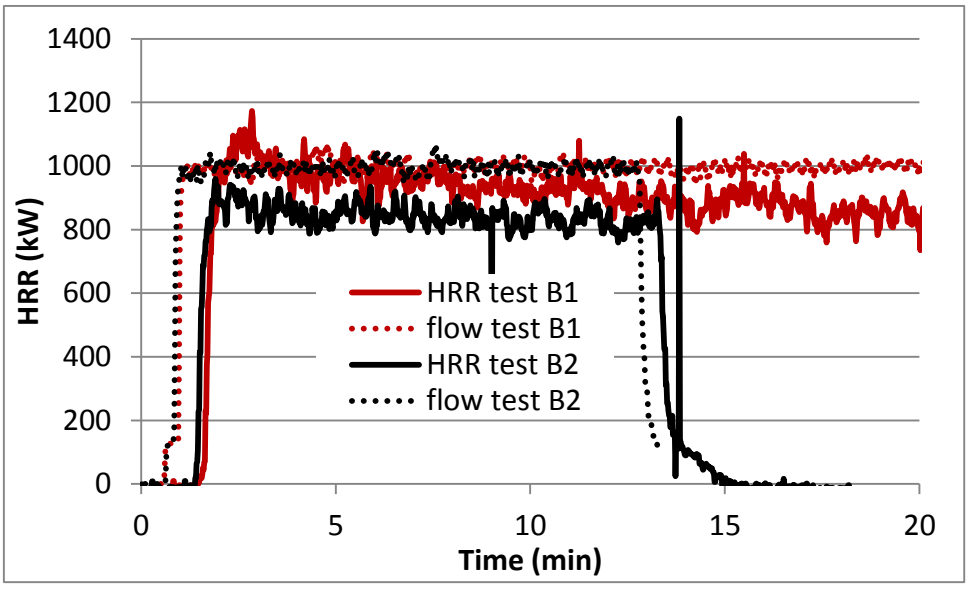

Figure 64. Comparison of the HRR as measured by the flow of propane (dotted lines) and by the oxygen consumption calorimetry (solid lines) between tests B1 and B2.

For tests D1 and D2, where the insulation is on the outside of the steel we cannot see any differences in the HRR between D1 and D2.

5 Conclusions

The purpose of this report is to describe the experiments behind the data to be referred to in later publications and to provide data available for other researchers to use in their developments of fire models. All data is available to download for free (Sjöström & Wickström, 2016). If any problems with the data occurs please contact the first author at johan.sjostrom@sp.se.

The data shows that the thermal properties of the surrounding structures have a great impact on the fire temperature development and on the fire exposure to the walls. The differences are also observed depending on how temperatures are probed, using PTs or TCs. The various measurements make the data series very useful for validation of fire models.

There are large differences in the fire exposure to the walls. The differences lies in both where and how the temperatures are probed but mostly what type of material the wall is made of. Using the thermal properties of the wall has a great impact which makes these data series a good tools for model developers to use and apply their model to.

6 Acknowledgement

Brandforsk, The Swedish Fire Research Board is gratefully acknowledged for financial support through project no. 307-131, Development and validation of simple and practical models from calculation of fire gas temperatures in enclosures.

7 Bibliography

Byström, A. (2013). *Fire temperature development in enclosures: Some theoretical and experimental studies.* Luleå: Luleå Technical University.

Byström, A., Sjöström, J., Anderson, J., & Wickström, U. (2016). *Validation of a one-zone room fire model with well-defined experiments.* Luleå: Luleå Technical University.

ENV 1991:1-2. (1995). *EUROCODE 1: Basis of Design and Actions on Sttructures. Part 1.2: Actions on Structures Exposed to Fire.* Brussels: European Comittee for Standardization.

Evegren, F., & Wickström, U. (2015). New approach to estimate temperatures in pre-flashover fires : Lumped heat case. *Fire Safety Journal, 72*, 77-86.

Gustafsson, S. E. (1991). Transient plane source techniques for thermal conductivity and thermal diffusivity measurements of solid materials. *Review of Scientific Instruments, 62*, 797.

Ingason, H., Appel, G., Li, Y., Lundström, U., & Becker, C. (2014). Large scale fire tests with a Fixed Fire Fighting System (FFFS). *The 6th International Symposium on Tunnel Safety and Security .* Marseille.

Jones, W. W. (1983). *A Review of Compartment Fire Models PB-83-208173.* Gaithersburg: National Bureau of Standards.

Karlsson, B., & Quintiere, J. G. (2000). *Enclosure Fire Dynamics.* Boca Raton: CRC Press LLC.

Magnusson, S. E., & Thelandersson, S. (1970). Temperature-Time Curves for the Complete Process of Fire Development - A Theoretical Study of Wood Fuels in Enclosed Spaces. *Acta Polytechnica Scandinavia*, p. Ci 65.

McGrattan, K. B., Baum, H. R., & Rehm, R. G. (1998). Large eddy simulations of smoke movement. *Fire Safety Journal, 30*, 161-178.

McGrattan, K., Peacock, R., & Overholt, K. (2014). Validation of Fire Models Applied to Nuclear Power Plant Safety. *Fire Technology*.

Mowrer, F. W. (1992). Closed-Form Estimate of Fire-Induced Ventilation Through Single Rectangular Wall Openings,. *Journal of Fire Protection Engineering*, 105-116.

Sjöström, J., & Andersson, P. (2013). *SP Report 2013:61 Thermal exposure from burning leaks on LNG hoses: experimental results.* Borås: SP Technical Research Institute of Sweden.

Sjöström, J., & Jansson, R. (2012). Measuring Thermal MAterial Properties fro structural fire engineering. *15th International Conference on Experimental Mechanics*, (p. 2846). Porto.

Sjöström, J., & Wickström, U. (2013). DIFFERENT TYPES OF PLATE THERMOMETERS FOR MEASURING INCIDENT RADIANT HEAT FLUX AND ADIABATIC SURFACE TEMPERATURE. *Proceeding of Interflam 2013* (p. 363). London: Interscience Communications Ltd.

Sjöström, J., & Wickström, U. (2016, 06 09). Dataset: Validation data for room fire models. DOI: 10.13140/RG.2.1.5138.6482. Retrieved 06 09, 2016, from https://www.researchgate.net/publication/303862845_Validation_data_for_room_fire_models

Sjöström, J., Amon, F., Appel, G., & Persson, H. (2015). Thermal exposure from large scale ethanol fuel pool fires. *Fire Safety Journal, 78*, 229-237.

Wade, C. A. (2008). *BRANZFIRE 2008 Compilaition of Verification Data.* Porirua: Branz.

Wickström, U. (1985). Application of the Standard Curve for Expressing Natural Fires for Design Purposes. In T. Z. Harmathy, *Fire Safety: Science and Engineering, ASTM STP882* (pp. 145-159). Philadelphia: American Society of Testing and Materials.

Wickström, U. (2016). *Temperature Calculations in Fire Engineering.* Springer International Publishing.

SP Technical Research Institute of Sweden

Our work is concentrated on innovation and the development of value-adding technology. Using Sweden's most extensive and advanced resources for technical evaluation, measurement technology, research and development, we make an important contribution to the competitiveness and sustainable development of industry. Research is carried out in close conjunction with universities and institutes of technology, to the benefit of a customer base of about 10000 organisations, ranging from start-up companies developing new technologies or new ideas to international groups.

SP Technical Research Institute of Sweden
Box 857, SE-501 15 BORÅS, SWEDEN
Telephone: +46 10 516 50 00, Telefax: +46 33 13 55 02
E-mail: info@sp.se, Internet: www.sp.se
www.sp.se

SP Report 2016:54
ISBN 978-91-88349-56-9
ISSN 0284-5172

More information about publications published by SP:
www.sp.se/publ

PART OF RI.SE

LULEÅ TEKNISKA UNIVERSITET

Department of Civil, Enviromental and
Natural Resources Engineering
Luleå University oc Technology, SE
SE-971 87 Luleå, Sweden

http://www.ltu.se
Telephone: +46 920-49 10 00
Fax: +46 920-49 13 99

OUR SPONSORS & PARTNERS:

Brandforsk

SP your Science Partner

RAPPORTER UTGIVNA AV BRANDFORSK 2016:

2016:1 Utrymning i långa trappor uppåt: Utmattning, gånghastighet och beteende

2016:2 Förflyttning vid utrymning

2016:3 Dubbelglasfasader - En brandteknisk förstudie

2016:4 Utveckling och validering av enkla och praktiska modeller för beräkning av brandgastemperaturer i rum/brandceller

2016:5 Brandskyddsfärgens funktion vid riktiga bränder

2016:6 Detaljutformning av moderna betongkonstruktioner för att förbättra brandmotståndet

1979 bildades Brandforsk som svar på behovet av ett gemensamt organ för att initiera och finansiera forskning och utveckling inom brandsäkerhetsområdet.

Brandforsk är statens, försäkringsbranschens och industrins gemensamma organ för att initiera, bekosta och följa upp olika slag av brandforskning.

Huvudman för Brandforsk är Brandskyddsföreningen och verksamheten leds av en styrelse och bedrivs i form av projekt vid universitet och högskolor, forskningsinstitut, myndigheter och företag.

Brandforsk

Årstaängsvägen 21 c
Box 472 44, 100 74 Stockholm
Tel: 08-588 474 14
brandforsk@brandskyddsforeningen.se